Chapter 6

Flocculation Dynamics of Mud: Sand Mixed Suspensions

Andrew J. Manning, Jeremy R. Spearman,
Richard J.S. Whitehouse, Emma L. Pidduck,
John V. Baugh and Kate L. Spencer

Additional information is available at the end of the chapter

http://dx.doi.org/10.5772/55233

1. Introduction

Sediments present in muddy estuaries and tidal inlets are regarded as being predominantly cohesive. These muds are usually composed of both clay and silt minerals combined with organic matter (Winterwerp and van Kesteren, 2004), and with the exception of very low particle concentrations or extremely high energy flow conditions, muddy particles occur as a spectra of floc sizes (D) when entrained into suspension (Kranck and Milligan, 1992).

In reality, natural sediments tend to comprise a mixture of different particle sizes, non-cohesive sediment including fine sands and, because of the interaction between these different fractions, the mixture behaves in a different way than the constituent parts (Whitehouse et al., 2000). Uncles et al. (1998) found that the proportion of mud and sand in subtidal and intertidal sediments can vary both temporally and spatially (e.g. Uncles et al, 1998). Fig. 1 shows an example of mud and sand in close proximity in the Eden Estuary (east coast of Scotland).

Very little is quantitatively known about how mixtures of cohesive and non-cohesive sediments, of different ratios and concentrations, interact whilst in suspension in turbulent flows and the effect this has on the resultant flocs formed and their flocculation properties, in particular the settling velocity. This has important implications for sediment transport modelling. Drawing on key literature and new data, this chapter will provide an overview of mixed sediment flocculation dynamics and how they can influence sediment transport.

The first part of this chapter reviews the theoretical aspects relating to the flocculation of mud:sand mixtures. It commences with a brief review of flocculation processes (2), followed by an overview of segregation environments verses flocculating suspensions (3), and then the biological influences on mixed sediment flocculation are summarised (4). The second part of

Figure 1. Sand and muddy sediments in close proximity, Eden Estuary, Fife (east coast of Scotland).

the chapter (5-7) draws on the findings of recent empirical studies assessing mixed sediment floc behaviour. The laboratory experimental protocols and findings are reported with floc data in spectral and parameterised formats presented and discussed. The potential implications of mud:sand flocculation on sediment transport modelling are also discussed (8-9).

2. Flocculation factors

From a sediment transport perspective, knowledge of the settling rate of sediments in suspension is vital in determining depositional fluxes and sediment transport rates. Sand is a non-cohesive material and therefore does not flocculate in pure sand suspensions. The settling velocity (Ws) is generally proportional to the square of the particle size or diameter (D). Conversely, mud is strongly cohesive and flocculates forming small, compact microflocs as well as larger, more porous macroflocs (Eisma, 1986; Manning, 2001; Manning and Dyer, 2002a,b) – Fig. 2. Flocculation is a dynamically active process which readily reacts to changes in hydrodynamically generated turbulent shear stresses (τ) (e.g. Krone, 1962; Parker et al., 1972; McCave, 1984; van Leussen, 1994; Winterwerp, 1998; Manning, 2004a), suspended particulate matter (SPM) concentration, together with salinity, mineralogy and biological stickiness.

http://dx.doi.org/10.5772/55233

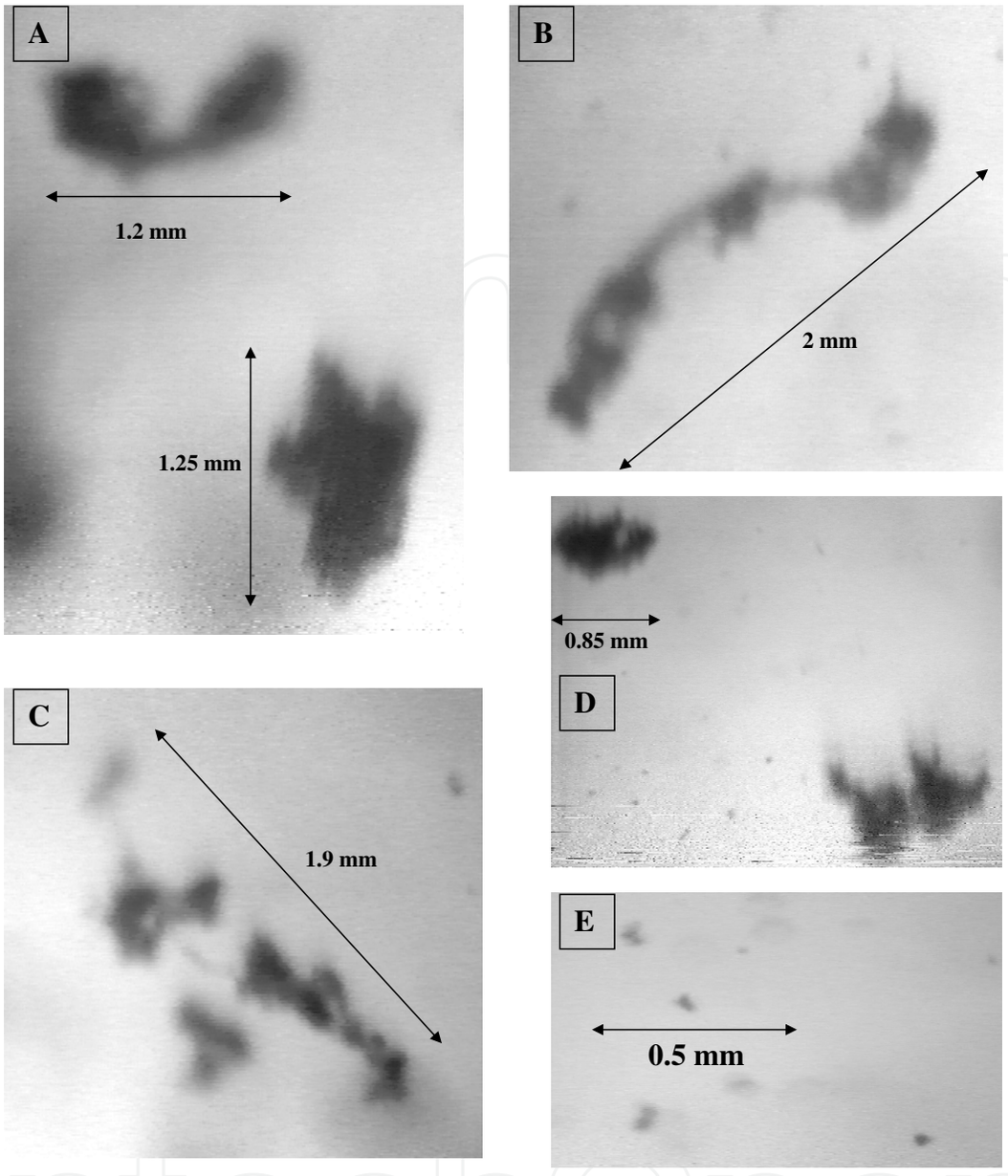

Figure 2. A selection of floc images from a predominantly muddy origin. A) A ragged cluster-type macrofloc (top) and a simple stringer composed of two macroflocs interlinked by organic fibres (bottom); B) a 'string of pearls' type macrofloc; C) a long interlinked stringer comprising two clustered macroflocs; D) ragged macroflocs settling; and E) a selection of small slow settling microflocs, some of which are probably the result of macrofloc fracturing and subsequent break-up during a turbulent event which exceeded the original macrofloc structural integrity threshold.

Flocculation can significantly alter the sediment transport patterns throughout an estuary, and floc properties can vary both in time and space. For example, Manning et al. (2006) showed that during spring tidal conditions in the Tamar Estuary (UK), macroflocs can typically reach 1-2 mm in diameter. These flocs demonstrate settling velocities up to 20 $mm.s^{-1}$, but their effective densities ϱ_e (i.e. the floc bulk density less the water density) are generally less than 50 $kg.m^{-3}$, which means they are prone to break-up when settling through a region of high turbulent shear.

There are, however, many estuarial environments where mud and fine sand co-exist as a single mixture (Mitchener et al., 1996) and this creates the potential for these two fractions to combine and exhibit some degree of interactive flocculation (Manning et al., 2007, 2009). The erosion and consolidation of mixtures of mud and sand has been thoroughly reviewed (Williamson, 1991; and Whitehouse et al, 2000), and there have been some studies that have examined mixed sediment settling (e.g. Dankers et al., 2007). However, very little investigation has been devoted to the potential flocculation that may occur when mud and sand mixtures are entrained into suspension, as it was not considered to be an important factor. This could be a valid assumption for a segregational environment, where the mud and sand do not combine into a single matrix.

When we refer to 'mixed sediment flocculation' in this chapter, we are primarily referring to suspension mixtures of mud (typically composed of clay minerals and fine silts up to 63 μm in diameter together with organic matter) and predominantly non-cohesive sediments (typically up to the size of fine sands, i.e. about 100-200 μm, as larger grains are unlikely to directly interact with mud).

Previous research has shown that a clay content of between 5 – 10% can cause natural sediment mixtures to behave in a cohesive manner (Dyer, 1986; Raudviki, 1998). Thus, different ratios of mud and sand can vary the level of cohesion, which will influence the resultant level of flocculation. Biological activity, more commonly associated with cohesive sediments, has been highlighted to play an important role in the cohesion of sediments (e.g. Paterson and Hagerthey, 2001). However, it is extremely difficult to quantify such a complex sedimentary matrix in a fundamental manner, primarily as a result of a lack of verification data.

Of the various processes that occur during a tidal cycle, flocculation of the sediment is regarded as one of the primary mechanisms that can affect the deposition, erosion and consolidation rates. An individual floc may comprise up to 10^6 individual particulates. As flocs grow in size their effective densities generally decrease (Koglin, 1977; Tambo and Watanabe, 1979; Klimpel and Hogg, 1986) and their settling speeds rise due to a Stokes' Law relationship (Dyer and Manning, 1998) between D and Ws. Furthermore, low density flocs also demonstrate settling velocities that are significantly quicker than the individual cohesive particles (~ 1-5 μm in diameter). The cohesive nature of these particulates is a combination of both the electrostatic charging of the clay minerals as they pass through brackish to highly saline water, and various sticky biogenic coatings, such as mucopolysaccharides (e.g. Paterson 1989).

Van Leussen (1988) theoretically assessed the comparative influence of the three main collision mechanisms: Brownian motion, turbulent shear and differential settling, and deduced that turbulent shear stresses, principally those generated by velocity gradients present in an estuarine water column, were the dominant flocculation mechanism. This mechanism was deemed most effective for turbulent shear stresses ranging between 0.03-0.8 Pa. These stresses are representative of those typically experienced in the near bed region of many European macrotidal and mesotidal estuaries and hence estuaries are ideal environments for flocculation.

The energy for turbulent mixing is derived from the kinetic energy dissipated by the water flowing across the sediment bed. The frictional force exerted by the flow per unit area of the

http://dx.doi.org/10.5772/55233

bed is the shear stress (turbulent shear stress during turbulent flow conditions). The efficiency with which the particles flocculate is a reflection of the stability of the suspension (van Leussen, 1994). A suspension is classified as unstable when it becomes fully flocculated, and is stable when all particles remain as individual entities.

As low to medium levels of turbulent shear stress can promote floc growth, high levels of turbulence that occur during a tidal cycle, can cause disruption to the flocculation process by instigating floc break-up, and eventually pull the constituent components of a floc apart. As turbulent activity increases, both turbulent pressure differences and turbulent shear stresses in the flow rise. If the floc structural integrity is less than the imposing turbulent induced forces, the floc will fracture. Also, aggregate break-up can occur as a result of high impact particle collisions during very turbulent events. Floc break-up by three-particle collisions tends to be the most effective (Burban et al., 1989). Hence, turbulent shear stress can impose a maximum floc size restriction on a floc population in tidal waters (McCave, 1984). Eisma (1986) observed a general agreement between the maximum floc size and the smallest turbulent eddies as categorised by Kolmogorov (1941a, b).

3. Segregation and flocculation

This section looks at how mud and sand can co-exist within an aquatic environment. Mud:sand sediment mixtures may behave either in a segregated way, or interact through flocculation. The phenomenon of mud:sand segregation considers the mud and sand to operate as two independent suspensions (van Ledden, 2002) and, as such, very little bonding occurs, and flocculation interactions between the cohesive and non-cohesive sediment fractions are non-existent. Mixed sediment experiments have shown that mud particles and sand grains which behave in a segregated manner, settle simultaneously but as independent fractions to form two well sorted layers at the bed/water interface (Ockenden and Delo, 1991; Migniot, 1968; Williamson and Ockenden, 1993).

Williamson (1991) reviewed a number of the characteristics of mud:sand mixtures in the natural environment (some of the key findings are summarised in this paragraph). The review investigated the distributions and characteristics of mud and sand mixtures based on a literature search and a review of relevant fieldwork data. Some of the features common to both mud and sand, such as: spatial distributions, vertical layering, bioturbation, depositional characteristics and flocculation, were described. The review suggested that muddier sediments were generally found in regions of lower dynamic activity and sandier sediments in higher energy regions. However, the local distributions could only be explained by local hydrodynamic analysis and these data were often lacking, which did not allow a complete picture to be obtained. Flocculation and the effects of salinity distributions were found to be important in governing the mud distributions, with a muddy reach often being found in the flocculation zone. The vertical profile of settled mud and sand was also investigated, with laminations of mud and sand often being found. The thickness of the layers in the laminated sediment profiles were typically sub-millimetre to a few millimetres. The process of bioturbation (i.e. the

reworking of the bed sediments by living organisms) can potentially produce a mixing of bed sediment particles prior to resuspension (e.g. Nowell et al., 1981; Paterson et al., 1990; Widdows et al., 2004). Thus a bed which is initially deposited as a discretely segregated layering of mud and sand may be transformed into a quasi-homogeneous mixture.

Van Ledden (2003) states that mud and sand can be deposited as mixtures or in alternating layers in estuaries. An example of this is visible in the upper part of Fig 1. Additionally, biological activity such as bioturbation (i.e. the reworking of the bed sediments), can mix the sediment particles. As a result the mud content in many parts of an estuary may not be uniform, but can become segregated both vertically and horizontally – a phenomenon known as mud:sand segregation (van Ledden, 2003).

Mud:sand segregation can have a direct influence on the settling velocity of the sediments once entrained. For instance, the settling velocity of individual sand grains could be reduced as they pass through a layer of flocculating muddy sediments in close proximity to the sea bed. Van Ledden (2003) provides three examples which illustrate the importance of why a physical understanding of the distribution of mud and sand in estuarine systems is important:

- Large mud content variations at the bed surface indicate that both mud and sand contribute to bed level changes in estuaries and tidal inlets. These will affect the navigable depth and high water levels.
- Cohesive muddy sediments have the propensity to adsorb contaminants (Förstner and Wittmann,1983). This, in turn, has a direct effect on water quality and related environmental issues (e.g. Uncles et al., 1998). The amount of segregation present on both temporal and spatial scales will provide an indication to the potential degree of pollution in bed sediments.
- The mud content in sediment beds is a crucial habitat parameter, which controls the distribution of flora and fauna in estuarine systems (e.g. Reid and Wood, 1976; Kennish, 1986; Widdows et al., 2004). Dyer et al. (2000), for example, showed that the sediment type and grain size are the best physical descriptors of floral and faunal assemblages in the upper zone of intertidal mudflats.

Van Wijngaarden (2002a, 2002b) examined the mud:sand content distributions in the upper 300 mm of the bed in the Haringvliet – Holland Diep (The Netherlands). Mud content varied from less than 15% at the mouths of most of the river branches feeding into the system, to nearly two thirds mud in the channels of the Holland Diep. Fast settling sand grains accumulated at the end of river branches whereas the slower-settling muddy suspensions were transported further downstream due to settling lag into the central part of the Holland Diep. The segregation is, to a large extent related to varying bed levels throughout the system and variations in the turbulent shear stresses (van Ledden, 2003), which influence erosion, deposition and transport.

There are also many locations where mud and sand co-exist as a mixture (Mitchener et al., 1996) and this creates the potential for these two fractions to combine within a flocculation matrix when re-entrained into suspension (Manning et al., 2007). When sand is added to a predominantly muddy matrix, Mitchener et al. (1996) found that this increased the binding

http://dx.doi.org/10.5772/55233

potential between the clay particles, for example as found in the subtidal mud patches off Sellafield in the Irish Sea (Feates and Mitchener, 1998). Thus the physical effect of adding cohesive mud to a sandy environment can create increased bed stability, which can potentially lead to mixed sediment flocs forming when the eroded bed is entrained (Kamphuis and Hall, 1983; Alvarez-Hernandez, 1990; Williamson and Ockenden, 1993; Torfs, 1994; Mitchener et al., 1996; and Panagiotopoulus et al., 1997). Even where sand and mud are considered to be fairly well segregated at the bed, sand and mud can co-exist in suspended sediment transport. Spearman et al. (2011) describe an example in the outer Thames Estuary (UK), renowned for being a sandy area, where the flux of suspended sediment of mud and sand are of the same magnitude.

Therefore, in a segregated environment, both mud and sand are present acting in a completely independent manner. In a flocculating environment, the mud and sand particles are interacting to form flocs which demonstrate very different characteristics (e.g. D, Ws, ϱ_e) from their compositional base. The nature of the sedimentary regime is best determined by observational measurements rather than being able to be determined *a priori*. This can pose additional problems for the prediction and modelling of suspended sediment transport in mixed sediment estuarine environments and this will be considered in Section 9.

4. Role of biology in mud: Sand mixtures

Although not directly examined in the laboratory experiments which will be discussed later in this chapter, it is important to consider other effects of which a key one is due to biological factors influencing the grains in suspension. These factors work in addition to the primary chemico-physical ones to make mixed sediment flocculation possible. In predominantly muddy/silty environments, benthic microphytobenthos contribute up to half the total autotrophic production in an estuarine system (Underwood and Kromkamp, 1999; Cahoon, 1999). Biostabilisation can increase particle cohesion, for example: epipelic diatoms (e.g. Paterson and Hagerthey, 2001) secrete extra-cellular polymeric substances (EPS; Tolhurst et al., 2002) as they move within the sediments. EPSs are regarded as highly effective stabilisers of muddy sediments (e.g. de Brouwer et al. 2005; Gerbersdorf et al. 2009; Grabowski et al., 2012).

The influence of biology on sand is reported to a much lesser extent in the literature, however sand grains that are exposed to long-term biological activity, may also develop a cohesive bio-coating which could increase the particle collision efficiency when they are entrained. Hickman and Round (1970) reported that sand particles can be joined by 'epipsammic' diatoms which attach to sand grains. Epipsammic macro-algal forms either adnate to the grain surface or attach to sand grains by their mucilage stalks. Epipsammic diatoms which are attached to sand grains, demonstrate strong adhesive properties to the grain surface (Harper and Harper, 1967). When fine sand and biology are combined into a single matrix, they can form “microbial mats” and the binding strength of these mats can be extremely high. Little (2000) states that because these types of algal threads are sticky with EPS, they can efficiently trap fine sand grains. These sticky bio-coatings can increase the collision efficiency (Edzwald and O’Melia,

1975) of particles when entrained into suspension, thus allowing fine sand grains to adhere with the clay fraction and form the cage-like structure around fine sand particles. Through microscopic photography, Wolanski (2007) observed the formation of large muddy flocs formed by mud creating a sticky membrane around large non-cohesive silt particles.

5. Experimental approaches

When investigating the role sand may play in the flocculation process, several important research questions need to be considered, including:

i. How does the settling velocity of mixed sediment flocs vary in response to different mud:sand mixtures?

ii. What effect does turbulence have on mixed sediment flocculation?

iii. Do resuspended sand particles favour interacting with microflocs or macroflocs more, and enhance their settling dynamics?

iv. If mixed sediment flocculation occurs, are sand grains directly incorporated into both microfloc and macrofloc fractions?

v. Does flocculation have an effect on the distribution of the particle mass and the mass settling flux (MSF) of different suspended mud:sand mixtures?

In order to address aspects of the above questions, a series of new controlled laboratory environment research were initiated to quantitatively examine the flocculation and interaction between suspended sand and mud sediment mixtures. Other aspects of mud:sand behaviour have been assessed in laboratory environment measurements (e.g. Ockenden and Delo, 1988; Williamson and Ockenden, 1993; Torfs, 1994; Torfs et al., 1996; Dankers et al., 2007). During the new experiments, suspensions of mud and sand, of different total concentrations, were sheared at different rates in a mini-annular flume and the resultant floc properties observed. The new experimental runs primarily comprised pre-determined mud:sand mixtures complemented with some additional data from naturally occurring mud:sand sediment mixtures.

5.1. Annular flume simulations

This study utilised a mini-annular flume to create a consistent and repeatable turbulent environment (see Fig. 3A) (Manning and Whitehouse, 2009). The annular flume has an outer diameter of 1.2 m, a channel width of 0.1 m and a maximum depth of 0.15 m, along with a detachable motor driven rotating roof (10 mm thick) to create the flow for cohesive sediment experiments (e.g. Manning and Dyer, 1999). Maximum flow speeds of approximately 0.7 $m.s^{-1}$ can be produced in the lower half of the water column, created by 10 mm deep paddles attached to the underside of the roof. A Nortek mini-ADV (Acoustic Doppler Velocimeter) probe was used to calibrate the flow in terms of velocity and turbulent kinetic energy (TKE) at a distance of 22 mm (the floc extraction height) above the flume channel base.

http://dx.doi.org/10.5772/55233

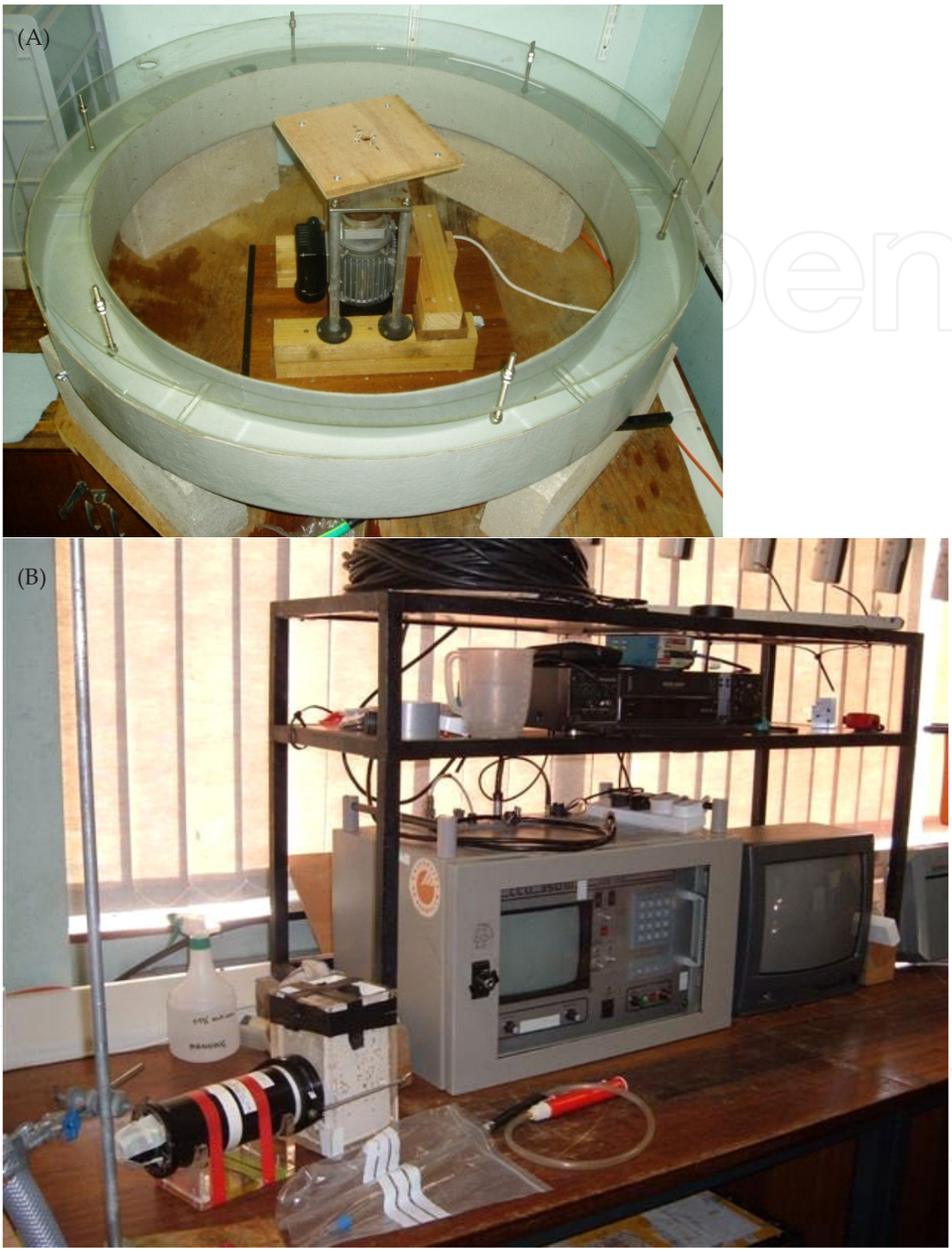

Figure 3. The mini-annular flume (A) and the LabSFLOC instrument set-up (B).

5.2. Floc property measurements

Representative floc populations were measured using the LabSFLOC version 1.0 – Laboratory Spectral Flocculation Characteristics – instrument (Manning, 2006). This utilises

a high magnification Puffin (model UTC 341) monochrome all-magnetic Pasecon tube video camera (Manning and Dyer, 2002a), to observe particles settling in a Perspex settling column (see Fig. 3B), allowing for minimal disruption of the particles. The video camera, positioned 75 mm above the base of the column, views all particles in the centre of the column that pass within a 1 mm depth of field, 45 mm from the lens. The video camera has an annulus of six high intensity red 130 mW LED's (light emitting diodes) positioned around the camera lens, which results in the flocs being viewed as silhouettes and produces a clear image of their size and structure. Whilst other studies may refer to muddy and/or mud-sand mixture particles as aggregates, for simplicity this study will refer to all aggregated combinations of particles as flocs.

5.3. Flume experimental protocols

The flume was filled with 45 litres of saline water (salinity = 20 ±0.2), to a depth of 0.13 m. The mixed sediments (both pre-determined and natural) were introduced into the flume as slurries of known SPM (suspended particulate matter) concentrations. Gravimetric analysis of extracted water samples was used to monitor the ambient concentration during the flume runs and check they were within the required experimental tolerances. For each run, different rotation speeds were used to shear the sediment slurries at shear stresses (τ) ranging from 0.06-0.9 Pa ±5% (equivalent Kolmogorov microscale values are: 381 - 138 μm ; equivalent G-values, the root mean square of the gradient in the turbulent velocity fluctuations, are: 7.1 – 54.2 s^{-1}) at the floc sampling point. Manning and Whitehouse (2009) report the calibration of the mini-flume hydrodynamics. Each run was initiated at the fastest rotational velocity and decreased towards the slowest speed as the run progressed. Further details of the experimental protocols are outlined by Manning et al. (2007).

The mixed sediment slurries were sheared in the flume for 30 minutes at each stress level. This duration of shearing, which was pre-determined in accordance with theoretical flocculation time (T_F), allowed each sediment suspension to attain floc equilibrium. Van Leussen (1994) defines T_F as the time required to decrease the number of individual unflocculated particles in a suspension, to just 10% of the initial number as a result of flocculation.

Floc population sampling comprised careful extraction of a suspension sample from the same height in the water column as the ADV calibration using a bespoke glass pipette. To obtain a floc sample, the rotation was stopped for approximately 6-8 seconds, although flow in the flume still continued through inertia, maintaining particles in suspension throughout this period. Manning and Whitehouse (2009) showed that the flow does not significantly slow until at least 15-20 seconds after stopping the drive motor. The floc sample was then transferred to the LabSFLOC Perspex settling column, whereby each individual floc was observed by the video camera as it was settling. Parameters of individual floc size (D) and settling velocity (Ws) were recorded during settling and the values obtained by video image post-processing. The experimental flow speeds generated in the flume were sufficient to keep the fine sand in suspension. The aperture of the pipette was brought into contact with the settling column water surface and held in place (vertically) allowing the captured flocs to undergo gravitational settling through the still

water column. Extensive testing of this sampling protocol during the EC COSINUS project (e.g. Gratiot and Manning, 2004) revealed that this technique created minimal floc disruption during acquisition. Once floc samples were extracted, the flume lid rotation continued at the next selected velocity.

5.4. LabSFLOC data processing

Parameters D and Ws, for all settling flocs viewed by the LabSFLOC video camera (for each sample), were measured simultaneously from the video recordings. Digitisation of the calibrated images resulted in a pixel resolution of 6.3 μm to determine floc size and position, from which settling velocity is determined by analysis of sequential images at a sampling rate of 25 Hz. The effective density (ϱ_e) of each floc was calculated by applying Stokes' Law relationship; ϱ_e is the difference between the floc bulk density (ϱ_f) and the water density (ϱ_w). To apply Stokes' Law, it is assumed that each sampled floc that fell through the still water enclosed within the settling column was within the viscous Reynolds region; i.e. when the individual floc Reynolds number (R_e) was less than 0.5. For instances where R_e exceeded 0.5, the Oseen modification, as advocated by ten Brinke (1994), was applied in order to correct for the increased inertia during settling. It is assumed that the measured particle is spherical; that is, it is as 'deep' as the measured D size.

The observed flocs were measured within a reference volume of water. By implementing a sequence of algorithms, originally derived by Fennessy et al. (1997) and modified by Manning (2004b), the dry mass of a floc population could be compared with the measured SPM concentration. This provides an estimate of the efficiency of the sampling procedure, and yielded corresponding rates of MSF. By definition, the data obtained from LabSFLOC are both of qualitative and quantitative value.

The floc data is presented as individual scatterplots and also as spectral size-banded (SB) distributions of floc mass and MSF; SB1 represents microflocs less than 40 μm in size and SB12 are macroflocs greater than 640 μm in diameter. Sample mean values are quoted. To provide a quantitative framework for population comparisons, the macrofloc and microfloc range of properties were assessed (Eisma, 1986; Manning, 2001), as these parameters are often used in flocculation modelling. The demarcation point for the macrofloc:microfloc fractions was a floc size of 160 μm (Manning, 2001) and was chosen for two main reasons: i) this was found to be the most statistically significant separation point for the majority of the mixed sediment floc populations in terms of mass settling properties; ii) it also provides computational continuity with previously derived flocculation algorithms for pure mud suspensions, such as the Manning Floc Settling Velocity (MFSV) algorithms which describe floc settling at different concentrations within turbulent flow (Manning and Dyer, 2007). Strictly it should be noted that microflocs are cohesive sediment flocs resistant to break-up by shear, however, in this study, many pure sand particles fall within the microfloc size range. Therefore, in this chapter microflocs refer to the 'fine particle population' < 160 μm in diameter. The sand used in the tests also contains a fraction with grains greater than 160 μm (around 10% by mass). Therefore, the macrofloc fraction may also contain a number of pure sand grains.

5.5. Floc microstructure

In order to examine the floc internal microstructure (matrix) at a sub-micron level (1-2 nm; Buffle and Leppard, 1995), use of transmission electron microscopy (TEM) was employed in a separate series of experiments (see Spencer et al., 2010). In addition, energy dispersive spectroscopy (EDS) was used to provide the elemental composition of the floc components. Samples were prepared for TEM analysis by first stabilising the samples in glutaraldehyde and embedding the samples in Spurr resin. The samples were polymerised at 60 ºC overnight. Ultrathin sections of the polymerised resins (50 nm) were obtained by sectioning with a diamond knife mounted in an ultramicrotome (RMC Ultramicrotome MT-7) and were then mounted on formvar copper grids for analysis. The ultra-thin sections were then observed in transmission mode at an accelerating voltage of 80 kV using a JEOL 1200EXIITEMSCAN scanning transmission electron microscope (STEM). The scanning mode of the STEM was used to generate a microprobe beam for EDS of individual floc components in sections allowing observation of minerals across the aggregates. A Princeton Gamma Tech (PGT) Si[Li] X-ray detector and Imix multichannel analyser provided spectra of all elements, with an atomic number greater than 10, on a "per colloid" basis.

6. Experimental results

Sections 6.1-6.5 report findings from the laboratory studies with pre-determined (PD) mud:sand mixtures conducted by Manning et al. (2007). Sections 6.5-6.6 report a selection of tests on naturally occurring mud and sand mixtures (NM), and analysis of a mixed sediment microfloc internal structure, respectively.

6.1. Sediments (PD)

The sand used in the pre-determined mixtures was named Redhill 110, which is a well-rounded and closely graded silica sand used by HR Wallingford for model testing with mobile sediment beds. Redhill 110 has a d_{50} of about 110 μm, with a d_{10} of 70 μm and a d_{90} of approximately 170 μm (Redhill 110 size values quoted are from independent analysis conducted at HR Wallingford). The experimental mud sample was obtained from the surface down to a depth of about 50 mm from the Calstock region of the upper Tamar Estuary (UK) and had an average organic content of approximately 10%. Fitzpatrick (1991) found Tamar Estuary mud to be generally high in kaolinite clay minerals and Fennessy et al. (1994) also report microscopic fragments of Tourmaline and Hornblende minerals present in Calstock mud. This particular mud was used as its floc properties are widely reported from earlier studies (e.g. Manning and Dyer, 2002b ; Mory et al., 2002 ; Bass et al., 2006). The mud was collected only a few days before the flume experiments were conducted, and cold stored (frozen) in a wet form to maximise organic matter preservation.

http://dx.doi.org/10.5772/55233

6.2. Overview of experimental runs (PD)

These experiments comprised a series of three main flume runs, A to C, based on pre-determined mud:sand (M:S) ratios (i.e. Run A = 75M:25S, Run B = 50M:50S and Run C = 25M:75S; units expressed as percentages). These main runs were each divided into 12 minor runs (based on concentration). This produced a total of 36 mixed sediment floc spectral samples. Three nominal total SPM concentrations were used: 200 mg.l^{-1}, 1000 mg.l^{-1} and 5000 mg.l^{-1}. Four shear stresses were used per run and these were determined by the ADV records as nominal clearwater τ values of: 0.06, 0.35, 0.6 and 0.9 Pa. The experimental conditions are summarised in Table 1.

Run	Sample	Mud (%)	Sand (%)	τ (Pa)	SPM (mg/l)
A	1	75	25	0.9	200
A	2	75	25	0.6	200
A	3	75	25	0.35	200
A	4	75	25	0.06	200
A	5	75	25	0.9	1000
A	6	75	25	0.6	1000
A	7	75	25	0.35	1000
A	8	75	25	0.06	1000
A	9	75	25	0.9	5000
A	10	75	25	0.6	5000
A	11	75	25	0.35	5000
A	12	75	25	0.06	5000
B	1	50	50	0.9	200
B	2	50	50	0.6	200
B	3	50	50	0.35	200
B	4	50	50	0.06	200
B	5	50	50	0.9	1000
B	6	50	50	0.6	1000
B	7	50	50	0.35	1000
B	8	50	50	0.06	1000
B	9	50	50	0.9	5000
B	10	50	50	0.6	5000
B	11	50	50	0.35	5000
B	12	50	50	0.06	5000
C	1	25	75	0.9	200
C	2	25	75	0.6	200
C	3	25	75	0.35	200
C	4	25	75	0.06	200
C	5	25	75	0.9	1000
C	6	25	75	0.6	1000
C	7	25	75	0.35	1000
C	8	25	75	0.06	1000
C	9	25	75	0.9	5000
C	10	25	75	0.6	5000
C	11	25	75	0.35	5000
C	12	25	75	0.06	5000

Table 1. Overview of experimental runs & samples.

During a pilot study to design and refine experimental protocols on the floc population evolution of a few pre-selected slurries, observations indicated that at a τ of 0.06 Pa the sand in the upper part of the water column settled to the channel base. However, this preliminary inspection indicated that there was still sufficient fine sand in suspension in the lower half of the flume to maintain the nominal mud to sand ratio in the floc sampling region. Furthermore, during the pilot study, checks were made on mixture homogeneity during suspension and revealed a nominal 8% mixture deviation (in terms of the sand) for a 75% sand slurry, reducing to less than 5% for a 75M:25S mixture. These nominal deviations are deemed acceptable for these mixed sediment flocculation experiments, but are taken into consideration when interpreting the study results.

During the main flume run, the total suspended concentrations were monitored by gravimetric analysis of samples withdrawn at the floc sampling point. This analysis indicated that the 200 $mg.l^{-1}$ total SPM varied the least at ±3%; the higher 5000 $mg.l^{-1}$ varied by ±4.7%; and the 1000 $mg.l^{-1}$ slurry nominally varying by ±4.3% by the time of floc sampling. Therefore, these relatively small deviations demonstrate that the majority of the mixed sediment mass was remaining in suspension for the shearing duration. Therefore the floc population characteristics were related closely to the initial total concentrations and mud:sand ratios. Further details on the homogeneity of mud:sand mixing within the mini-annular flume is reported by Manning et al. (2009).

6.3. Floc size and settling velocity spectra with mixtures of mud and sand (PD)

To demonstrate the floc properties for suspensions comprising 75M:25S, 50M:50S and 25M:75S, a number of examples of the individual detailed spherical-equivalent dry mass weighted floc sizes vs. settling velocity spectra are presented (Figs 4Ai-4Av). The plots represent the mass-balance corrected floc distributions, thus an individual point on each graph may represent several flocs with very similar floc characteristics. The diagonal lines on each scatterplot represent contours of constant floc effective density, ϱ_e, (units = $kg.m^{-3}$), i.e. the bulk density minus the water density.

For completeness the full set of D vs. Ws floc distributions for all experiments can be found in Figs. 5, 6 and 7. By following the plots in each column, starting at the lower plot, one can track the evolution of the floc populations formed in a constant SPM concentration as the shear stress rises through the various increments. Similarly, by following the plots from left to right, the effect of rising concentration on the floc dynamics can be observed. Sections 6.3 and 6.4 summarise some of the key observations from a selection of the populations.

6.3.1. Run A (75M:25S) (Fig. 5)

The flocs from the lower SPM concentration (200 $mg.l^{-1}$), A1-A4, appear to produce three separate clusters: a sub-70 μm group, a fraction greater than 160 μm; with a third group sandwiched in between. For example, the 204 individual flocs that comprised sample A3 (Fig. 5 box A3) ranged from 42 μm to 182 μm in diameter (also Fig. 4Ai). Corresponding settling velocities spanned 0.3 $mm.s^{-1}$ to 3.4 $mm.s^{-1}$ for sample A3.

http://dx.doi.org/10.5772/55233

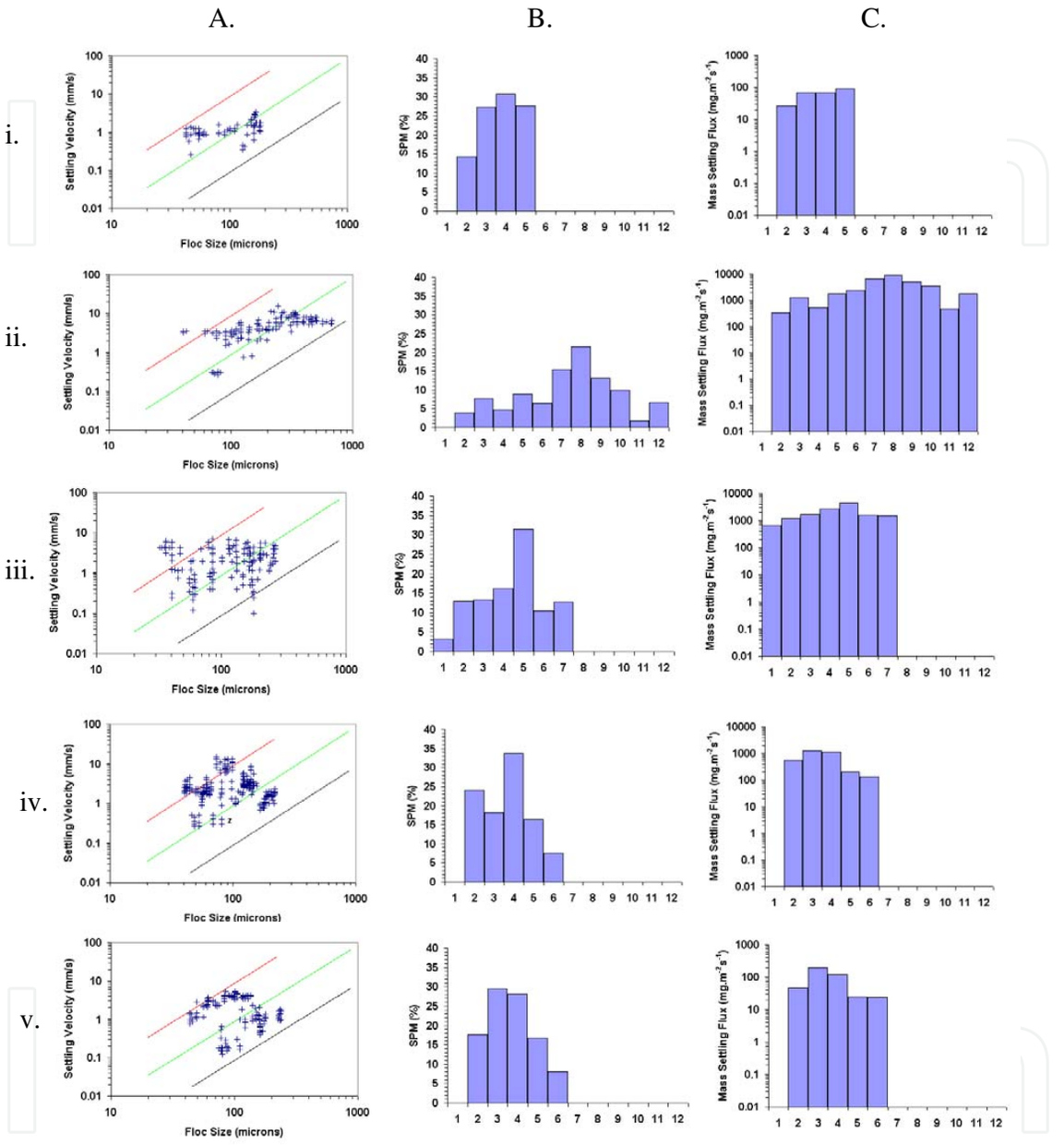

Size Band	1	2	3	4	5	6	7	8	9	10	11	12
Floc size (µm)	< 40	40 -80	80 -120	120 -160	160 -200	200 -240	240 -320	320 -400	400 -480	480 -560	560 -640	> 640

Figure 4. The floc size vs. settling velocity scatter plots (A, left-hand column) for five selected samples: i) A3, ii) A11, iii) B9, iv) C6 and v) C3. Diagonal lines on figures in column A represent contours of constant Stokes equivalent effective density: red = 1600 kgm^{-3}, green = 160 kgm^{-3}, and black = 16 kgm^{-3}. The centre (B) and right-hand (C) columns represent the corresponding size-banded SPM% and mass settling flux distributions (units = mg.m^{-2}s^{-1}). The size bands are illustrated in the table below the plots.

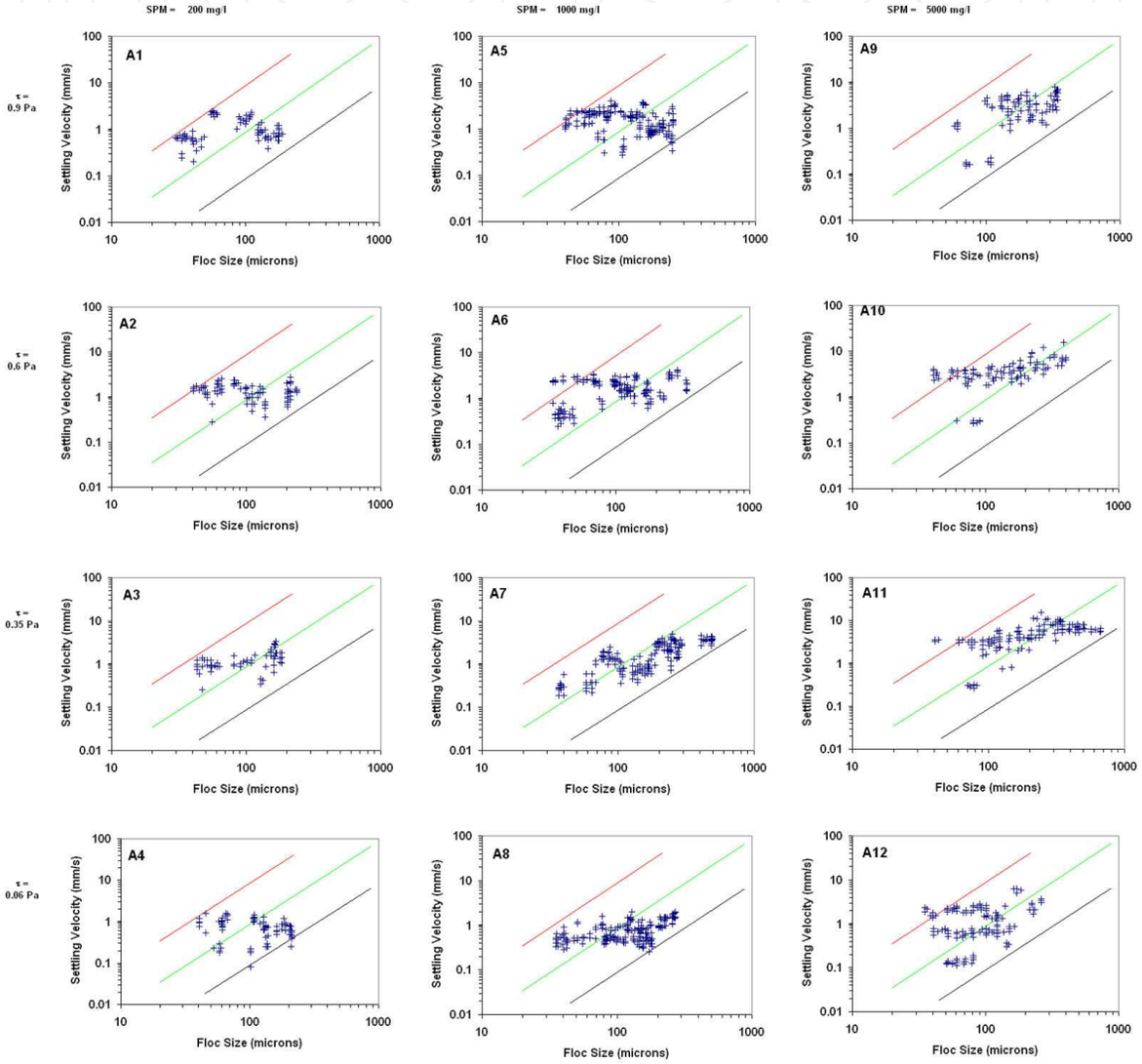

Figure 5. Distribution floc/aggregate size and settling velocity characteristics for the Run A (75M:25S) samples. Diagonal lines represent contours of constant Stokes equivalent effective density: red = 1600 kgm^{-3}, green = 160 kgm^{-3}, and black = 16 kgm^{-3}.

http://dx.doi.org/10.5772/55233

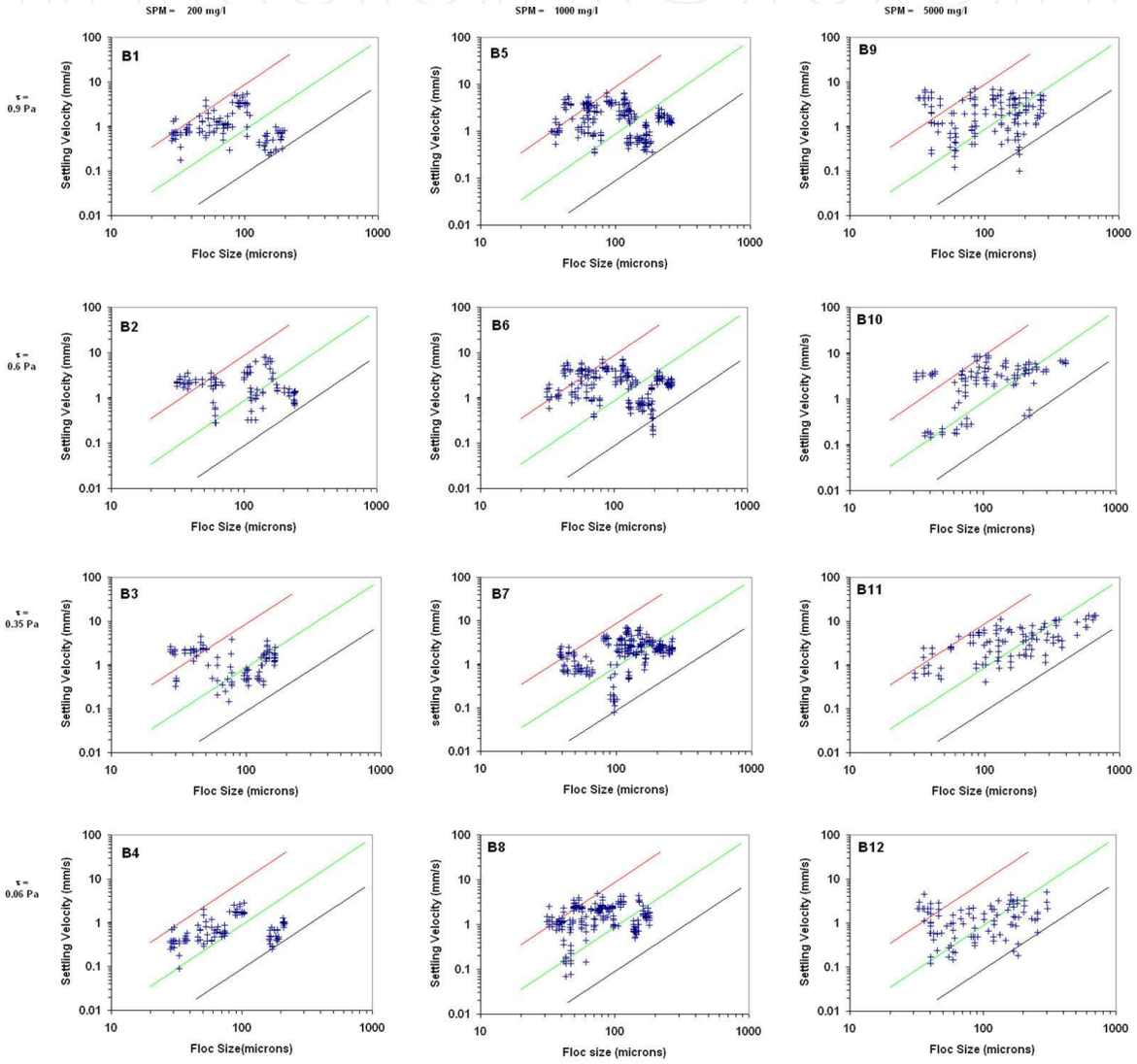

Figure 6. Distribution floc/aggregate size and settling velocity characteristics for the Run B (50M:50S) samples. Diagonal lines represent contours of constant Stokes equivalent effective density: red = 1600 kgm^{-3}, green = 160 kgm^{-3}, and black = 16 kgm^{-3}.

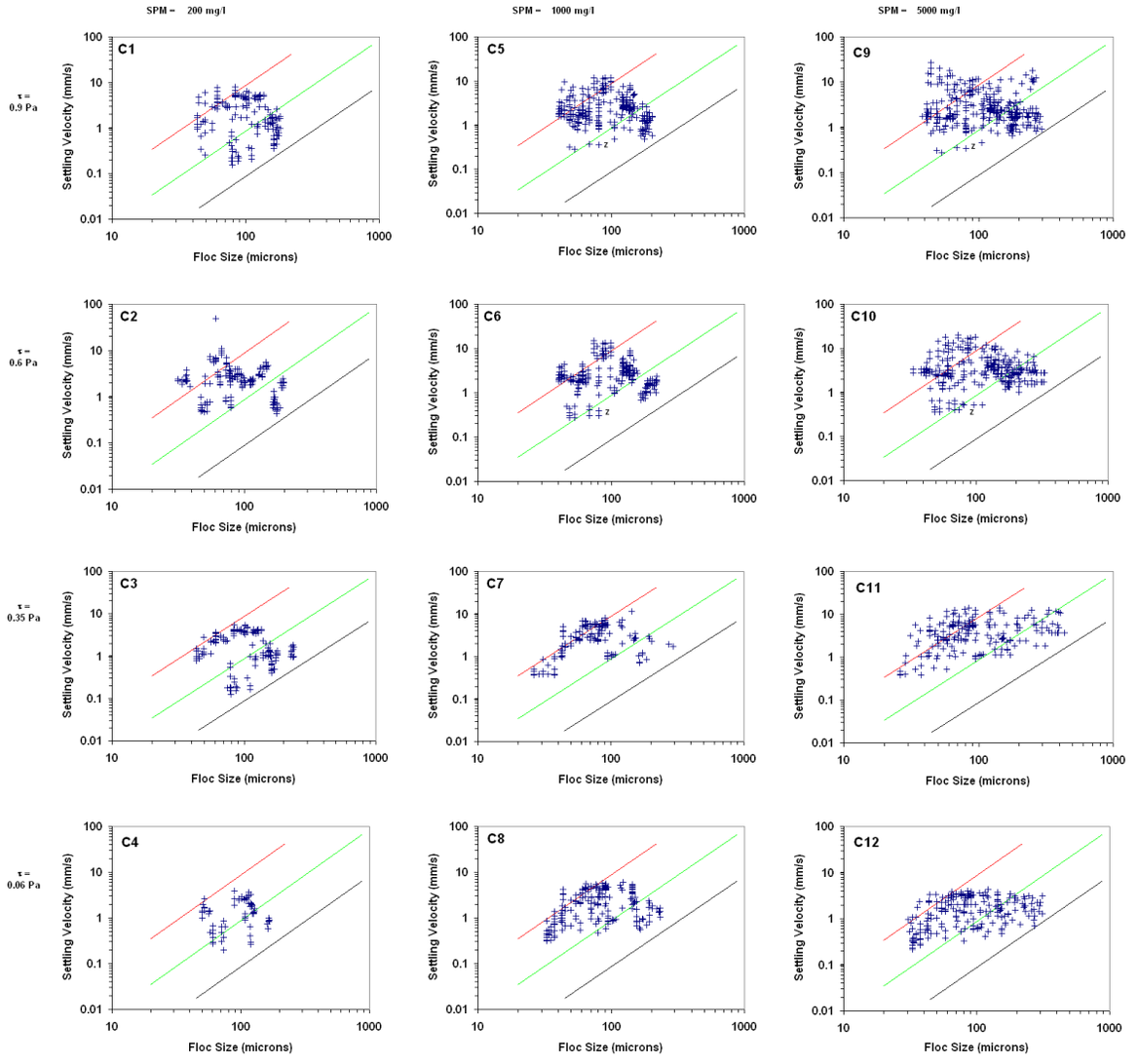

Figure 7. Distribution floc/aggregate size and settling velocity characteristics for the Run C (25M:75S) samples. Diagonal lines represent contours of constant Stokes equivalent effective density: red = 1600 kgm^{-3}, green = 160 kgm^{-3}, and black = 16 kgm^{-3}.

The Run A floc growth was potentially stimulated by a greater abundance of sediment, with D_{Max} (maximum floc diameter) nearly reaching 700 μm at peak turbidity (5000 mg.l^{-1}). The floc growth signified a corresponding quickening in Ws with rising SPM, producing Ws_{Max} (maximum settling velocities) of 7-8 mm.s^{-1} at 5000 mg.l^{-1}; approximately double the speed exhibited by the dilute sandy mud suspensions. This is demonstrated by A11 (Fig. 5 box A11 and Fig. 4Aii) where the shear stress was the same as A3 (0.35 Pa), but the particle mass in suspension were raised by a factor of twenty five. Flocs greater than 160 μm comprised 61% of the total population. In terms of the effects of shear stress, 0.35 Pa seems to produce the largest, fastest settling macroflocs at 75M:25S. These inter-relationships will be further examined in the Discussion (Section 7).

http://dx.doi.org/10.5772/55233

6.3.2. Run B (50M:50S) (Fig. 6)

Increasing the sand content to equal the mud fraction (50M:50S), brought about a general decrease in the macrofloc settling velocity across the entire shear stress range at each base concentration increment.

In contrast to the macroflocs, the smaller 50M:50S microfloc fractions all displayed quicker fall rates when compared to the 75% mud in settling rate for each mixed suspension run, with the 5000 $mg.l^{-1}$ 50M:50S mixed suspension (sample B9, Fig. 6) microfloc fraction settling velocity peaking at a highly turbulent τ of 0.9 Pa.

The B9 size vs. settling velocity floc scatter plot (Fig.6 box B9 and Fig. 4Aiii) shows a "W" or "double-V" pattern to the aggregates distribution. By this we mean there are small, fast settling microflocs (nominal 20-40 μm), whose settling velocity range expands at the mid-size microfloc fraction (nominal 40-80 μm). Then, for the microflocs nominally greater than 80 μm in size, the spread in the microfloc Ws again reduces, thus producing a "V" shaped distribution. This "V" pattern is repeated for the macroflocs, with their largest Ws scatter occurring between 185-230 μm for Sample B9.

The microflocs forming the first "V" spanned from 32 μm and up to 114 μm where they form the apex with the adjacent "V" to form the "W". At each end of the size range there are aggregates settling at 5-7 $mm.s^{-1}$, whilst the middle part of the "V" sections shows flocs falling as slowly as 0.1 $mm.s^{-1}$. In the upper left part of the D vs. Ws scatterplot, there are a number of aggregates which appear to be between 35-50 μm in diameter, settling at 3-6 $mm.s^{-1}$ and exhibiting effective densities of 2000-5000 $kg.m^{-3}$, which is up to three times the effective density of a sand grain. It is most probable that these are individual fragments of either Tourmaline or Hornblende; minerals native to the Tamar Estuary and its catchment. The majority of the aggregate population between 45-90 μm appears to be dominated by sand grains, with a minimum amount of cohesive matter (i.e. mud content) attached to the sand grains. These would form very basic, dense, lower order floc structures, which would trap very little interstitial water. This is indicated by high effective densities (ρ_e ~1200-1400 $kg.m^{-3}$), large fractal dimensions (nf of 2.8-2.9) and low porosities (~10-20%), but they are still not characteristic of pure (i.e. unflocculated) sand grains.

6.3.3. Run C (25M:75S) (Fig. 7)

Reducing the mud content to 25%, meant the microfloc size fraction tended to dominate the size and settling dynamics as the total concentration rose throughout Run C. At dilute conditions, the microflocs represented less than one quarter of the individual flocs for the A1-4 samples; for example C3 (Fig 7. Box C3 and Fig. 4Av). However, with many of the sub-160 μm C1-4 flocs settling at 4-7 $mm.s^{-1}$, they were falling significantly quicker than their muddier Runs A and B counterparts.

A five-fold rise in the total SPM concentration increased the production of smaller flocs, with the macrofloc size fractions only accounting for 10-20% of the individual aggregates. For example, nearly 90% of the C6 flocs (τ = 0.6 Pa, SPM = 1000 $mg.l^{-1}$) were within the microfloc range (Fig. 7 box C6 and Fig. 4Aiv). This was approximately 15-20% more microflocs when

compared to the more cohesive B6 and A6 samples (see relevant boxes in Fig. 6 and Fig 5. respectively).

The accuracy of effective density values is crucial to the determination of when mixed sediment particles are flocculating, or if the fine sand particles remain as individual inert entities. The reliability of the LabSFLOC effective density estimates are demonstrated by their observation of pure sand grains (Fig. 8). The D and Ws fine sand observations produce a distribution which closely follows the 1600 kg.m^{-3} density contour, generally not deviating by no more than ±100 kg.m^{-3} for over three hundred sand grain observations.

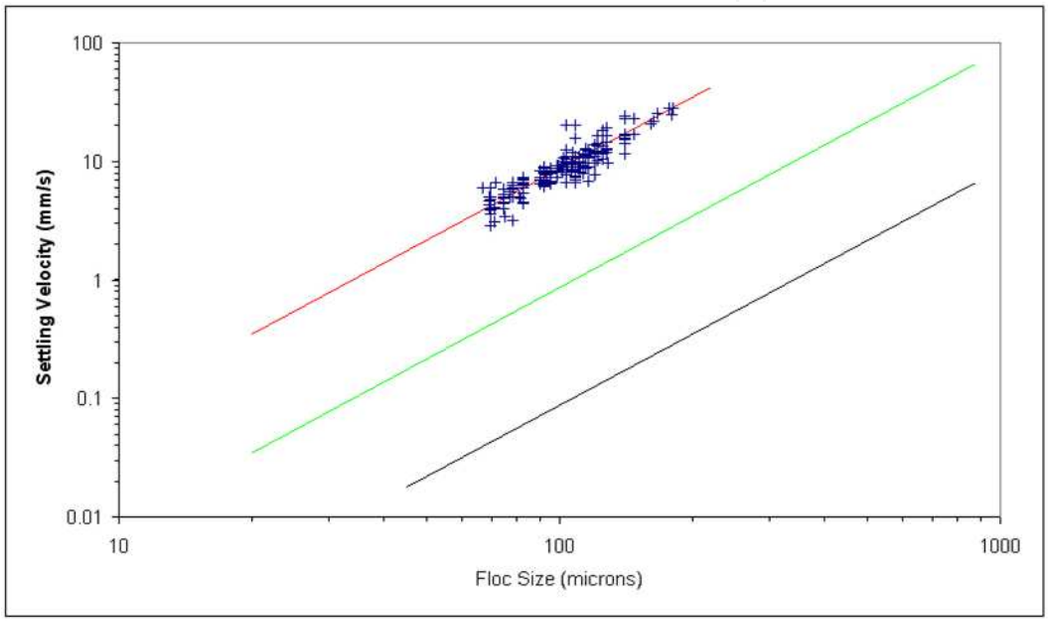

Figure 8. Settling settling vs. floc size for a 100% sand sample. Diagonal lines represent contours of constant Stokes equivalent effective density: red = 1600 kgm^{-3}, green = 160 kgm^{-3}, and black = 16 kgm^{-3}.

6.4. Floc composition with mixtures of mud and sand (PD)

To illustrate how the floc structure varies at different mud:sand ratios, a few examples will be presented with the compositional properties (effective density and SPM) as size band distributions. We start with sample A3 which represents a muddier dilute concentration and the D vs. Ws scatterplot (see Fig. 4Ai) shows that the macrofloc and microfloc fractions formed three distinctively separate groups. From Fig. 4Ai we can determine that the microfloc effective densities (ϱ_{e_micro} ranging from 200-1580 kg.m^{-3}) were generally an order of magnitude greater than the macroflocs (ϱ_{e_macro} from 30-100 kg.m^{-3}). This suggests that together with some individual sand grains, some of the sand grains may have also been included into the microfloc structure during the flocculation process.

In terms of the mass distribution across the dilute concentration floc population, the small microflocs for A3 represented three quarters of the mass (Fig. 4Bi). This is similar to fully cohesive suspensions within a moderately-high shear zone (τ of 0.6-1 Pa) which suggests the

http://dx.doi.org/10.5772/55233

mixture is still behaving as a cohesive suspension, even with 25% sand present in the initial mixture. For this sample, the denser, more compact microflocs represented two thirds of the total 254 $mg.m^{-2}s^{-1}$ mass settling flux (Fig. 4Ci).

At a concentration of 5000 $mg.l^{-1}$, the 75M:25S macroflocs of sample A11 (Fig. 4Aii) the macroflocs were observed to be delicate, low in density (ρ_e ranging from 20-200 $kg.m^{-3}$) entities. The A11 macroflocs now represented 84% of the mass (Fig. 4Bii), which was more than double the A3 macrofloc mass. Higher turbidity stimulated floc growth in A11, resulting in the largest flocs (D_{max}) growing to 670 μm.

The A11 microfloc fraction consisted of higher density flocs, with the smallest flocs (40-80 μm) demonstrating effective densities of over 1100 $kg.m^{-3}$, which are indicative of sand-laden microflocs or sand grains (where the effective density is greater than 1600 $kg.m^{-3}$). With sand accounting for one quarter of the total suspension and the microflocs representing 16% of the A11 mass, continuity of mass dictates that a reasonable portion of the sand must have been incorporated in many of the macrofloc structures during the flocculation process. This is very different from some segregational theories (e.g. van Ledden, 2003) which regard suspensions of sand and mud as completely independent entities.

Collectively, the fast settling A11 macroflocs contributed 94% of the total mass settling flux (33 $g.m^{-2}s^{-1}$; Fig. 4Cii); a result of a macrofloc settling velocity of 7.2 $mm.s^{-1}$, which was nearly three times quicker than the corresponding Ws_{micro}. To put this all into context, the A11 total MSF was 13 times greater than the value computed by the use of an estimated mean settling velocity of 0.5 $mm.s^{-1}$; a typical parameterised cohesive sediment Ws value derived from the gravimetric analysis of Owen tube (Owen, 1976) samples. Dearnaley, (1996) summarised the primary drawback associated with the Owen tube and other field settling tube devices, including the disruptive nature on flocs of the instrument sampling. Even the A11 microflocs were settling five times quicker than a 0.5 $mm.s^{-1}$ parameter value (A11 Ws_{micro} = 2.5 $mm.s^{-1}$).

Examination of the 50M:50S sample B9 D vs. Ws scatterplot (Fig. 4Aiii), reveals the presence of a high density sub-group of flocs (upper left-hand section). These flocs, which are only 35-50 μm in diameter, are settling at 3-6 mms^{-1} and exhibiting effective densities of up to 2000-3500 $kg.m^{-3}$. This is up to three times the typical effective density of a sand grain. It is proposed that these are individual fragments of either Tourmaline or Hornblende; minerals native to the Tamar Estuary and its catchment (Fennessy et al., 1994). However, given the Tamar's history for shipping copper out of Calstock, and the rich mining history for everything from tin to silver, these heavier particles could be from a number of sources. The majority of the floc population between 45-90 μm appears to be dominated by sand grains as their effective densities are typically greater than 1600 $kg.m^{-3}$, with a minimum amount of cohesive matter (i.e. mud content) attached to the sand grains. These would form very basic, dense, lower order floc structures, which would trap very little interstitial water. We could ask the question; if these high density particles were included in the mud used for all mixtures, why are they observed only in this case? It is possibly due to uncertainty made when estimating size and settling velocity of flocs rises as the particles become smaller (i.e. they are harder to detect as their images are formed from less pixels). Furthermore, these very dense mineral fragments only constitute a few percent of the total mass.

To reiterate, the microflocs tended to dominate the less cohesive Run C samples (25M:75S). The C6 (τ = 0.6 Pa and SPM = 1000 mg.l^{-1}) macroflocs did not grow larger than 215 μm (Fig. 4Aiv). This was a 40% reduction in size when compared to the corresponding 75M:25S sample (A6). The low density (effective densities of less than 70 kg.m^{-3}) C6 small macroflocs fell at a combined average Ws_{macro} of 1.35 mm.s^{-1}, whilst the Ws_{micro} was 3.6 mm.s^{-1}. The C6 microflocs also represented three quarters of the SPM and 90% of the C6 MSF of 3.2 g.m^{-2}s^{-1} (see Fig. 4Biv and Fig. 4Civ, respectively). To place this MSF observation into perspective: it was approximately double the flux produced either by pure mud or a 75% mixed mud suspension; 31% greater than a 50:50 mixture could produce, and six times greater than the flux obtained by using a constant 0.5 mm.s^{-1} Ws (a typical settling parameter used in cohesive sediment transport modelling).

The 'clustered' appearance depicted by the lower concentration (SPM = 200 mg.l^{-1}) 25M:75S C3 sample (Fig. 4Av) is similar to Sample C6 (Fig. 4Av). The shear stress was less turbulent (τ = 0.35 Pa) than C6, so one would assume the floc settling dynamics would improve. However, the removal of three quarters of the cohesive matter meant that the Ws_{macro} was only 0.9 mms^{-1}; half the Ws_{macro} for the 75M:25S run A3. As with the 1000 mg.l^{-1} C6 suspension, the C3 macroflocs only represented a quarter of the SPM (Fig. 4Bv). The main difference between the lower and the higher Run C suspension was fewer individual unflocculated sand grains in the suspension at the lower turbidity.

6.5. Analysis of macrofloc: Microfloc trends (PD)

This section will look at the macrofloc and microfloc (Eisma, 1986) settling velocity trends (i.e. Ws_{macro} and Ws_{micro} respectively) calculated from the pre-determined mud:sand mixture data presented earlier in Section 6.3. A dual-modal approach is advised when assessing parameterised floc settling and floc mass population data, as it tends to be more realistically representative than a single sample average (Dyer et al., 1996; Mietta, 2010), especially when considering the effects of mass settling fluxes to the bed (Baugh and Manning, 2007). This approach also permits quantitative inter-comparisons with previous pure mud flocculation studies.

The density contours superimposed on the Ws vs. D scatterplots presented in Section 6.3 indicate that only a minimum number of sand grains remained in an unflocculated state. This was confirmed from an assessment of both the effective density and SPM distributions. Therefore these few grains were included in the microfloc analysis presented in this section, as they form part of the total suspension and this provides the continuity of mass when comparing the different samples. However, to make these assessments fully rigorous, the mud fraction of the samples will be isolated and examined independently in the 'modelling implications' section (see Section 9).

6.5.1. Run a using 75% mud: 25% sand

Fig. 9 shows the macrofloc and microfloc averaged settling velocity plots which cover both the pre-determined mixtures experimental concentration and shear stress ranges. The solid lines

http://dx.doi.org/10.5772/55233

on Figs 9.A and 9.B correspond to the 25% sand mixed suspensions; the dotted curve lines are the contrasting 100% mud suspension outputs from the MFSV (this prediction was calibrated principally for Tamar mud extracted from the same study location). The straight dotted lines represent the d_{50} and d_{10} settling rates of pure sand grains determined by the *SandCalc* sediment transport computational software package (HR Wallingford, 1998).

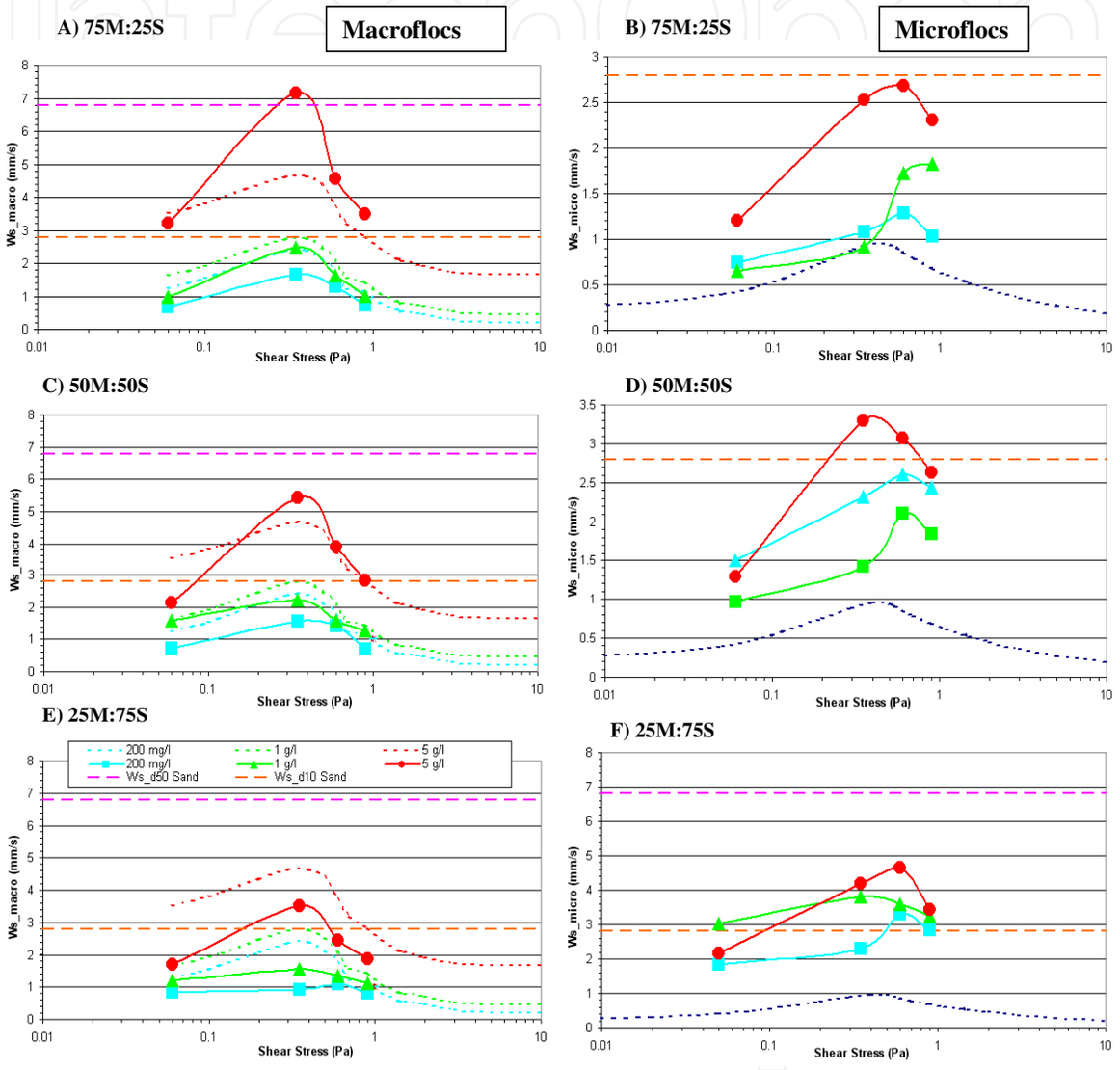

Figure 9. Ws_{macro} (left column, y-axis, units = $mm.s^{-1}$) & Ws_{micro} (right column, y-axis, units = $mm.s^{-1}$) values for runs A (75M:25S), B (50M:50S) and C (25M:75S), plotted against shear stress (x-axis, units = Pa). Solid lines + symbols indicate mixed sediment floc data points. Dashed lines indicate predicted behaviour of 100% mud macroflocs at three concentrations, and 100% mud microflocs at a single concentration. Lines indicating SandCalc estimated settling velocities of unhindered d_{10} and d_{50} pure sand grains are also plotted.

Substituting 25% of the pure mud suspension for sand produced a distinct change to the macrofloc settling velocity (Fig. 9.A). Starting at the lowest concentration (200 $mg.l^{-1}$), the quiescent conditions of 0.06 Pa only produced a Ws_{macro} of 0.65 $mm.s^{-1}$: nearly half the settling

rate of pure mud. As the shear stress increased, the floc dynamics respond and the settling velocity increased to a maximum of 1.7 $mm.s^{-1}$ at 0.35 Pa, which was 0.8 $mm.s^{-1}$ slower than pure mud at the same concentration. The intermediate concentration (1000 $mg.l^{-1}$) Ws_{macro} closely mimicked the settling profile of pure mud macroflocs at the less turbid 200 $mg.l^{-1}$. This is primarily a result of the 75M:25S suspension lacking sufficient cohesion because it only comprises 75% mud and the potential level of flocculation is more restricted than pure mud. The mixed sediment macroflocs also demonstrated lower effective densities (~30-50 $kg.m^{-3}$) than their pure mud counterparts.

The smaller mixed sediment microfloc fractions all settled faster than the pure mud equivalents, at each stress increment (Fig. 9.B). Where the macrofloc mixed fraction showed settling peaks at 0.35 Pa, similar to natural muds (Manning, 2004b), the mixed Ws_{micro} tended to produce a maximum at the higher turbulent shear stress of 0.6 Pa.

At high turbidity (5000 $mg.l^{-1}$), the macroflocs were nearly three time more dense than at lower turbidity. This saw the Ws_{macro} peaking at 7.2 $mm.s^{-1}$, which was 2.5 $mm.s^{-1}$ faster than the 100% mud equivalent, and 0.4 $mm.s^{-1}$ quicker than a d_{50} pure sand. The corresponding Ws_{micro} was 2.7 $mm.s^{-1}$, which was similar to a d_{10} sand grain and 1.7 $mm.s^{-1}$ quicker than pure mud microflocs.

6.5.2. Run B using 50% mud: 50% sand

Increasing the sand content to equal the mud fraction (50M:50S), brought about a general decrease in the macrofloc settling velocity across the entire shear stress range at each base concentration increment (Fig. 9.C). For the 200 $mg.l^{-1}$ slurries sheared at 0.35 Pa, the equally mixed sediment produced a Ws_{macro} of 1.6 $mm.s^{-1}$, a reduction of 0.1 $mm.s^{-1}$ from the 75% mud, and was 0.8 $mm.s^{-1}$ slower at settling than the pure mud benchmark.

At the highest suspended concentration (5000 $mg.l^{-1}$), and again at a turbulent stress of 0.35 Pa, the 50M:50S slurry produced a Ws_{macro} of 5.4 $mm.s^{-1}$. This was 0.8 $mm.s^{-1}$ faster than pure mud, but 1.8 $mm.s^{-1}$ slower than the 75M:25S macroflocs. This large Ws_{macro} difference exhibited between the 75M:25S and 50M:50S mixtures, decreased as the TKE dissipated to a lesser level. However, both mixed suspension macroflocs at the low shear stress were still slower than pure mud, which settled considerably faster.

In contrast to the macroflocs, the smaller 50M:50S microfloc fractions (Fig. 9.D) all displayed quicker settling velocities when compared to 75M:25S. The one main exception was the 5000 $mg.l^{-1}$ concentration, where Ws_{micro} achieved a maximum speed of 3.3 $mm.s^{-1}$; which was 2.3 $mm.s^{-1}$ faster than pure mud and 0.75 $mm.s^{-1}$ quicker than the corresponding 75M:25S microflocs.

6.5.3. Run C using 25%mud: 75% sand

The addition of a greater amount of sand particles in suspension significantly enhanced the settling dynamics at their respective shearing stresses which stimulate maximum flocculation. All 25M:75S values of Ws_{micro} exceeded the purely cohesive suspensions by more than a factor

http://dx.doi.org/10.5772/55233

of two (Fig. 9.F), and the majority of the microfloc samples also exceeded the settling rate of a d_{10} sand grain. At an SPM concentration of 200 mgl^{-1}, the Ws_{micro} at 0.06 Pa was 1.8 $mm.s^{-1}$ and increased to a peak of 3.3 $mm.s^{-1}$ at 0.6 Pa. By increasing the SPM concentration to 5000 $mg.l^{-1}$, the Ws_{micro} maximum peaked at 4.7 $mm.s^{-1}$. This was approximately five times faster than the value for 100% mud, and nearly double the equivalent 75M:25S Ws_{micro} (Fig. 9.F).

Conversely, all macrofloc fractions settled significantly slower within the less cohesive suspensions. At peak turbidity, the macrofloc fraction fell at 3.5 $mm.s^{-1}$; this was the sole macrofloc fraction to exceed the settling velocity of d_{10} sand. In fact, this 25M:75S macrofloc fraction was 1.2 $mm.s^{-1}$ slower than the corresponding Ws_{micro} from the same run.

In terms of the particle mass distribution: as the percentage content of non-cohesive sediment rose (i.e. mud content decreased), the relative contribution of the microfloc fraction to the total SPM concentration in each population increased.

6.6. Comparative data for sediment from Portsmouth Harbour – Natural Mixture (NM)

To support the data derived from the pre-determined mud:sand slurries, a selection of naturally occurring mixed sediment samples collected from within Portsmouth Harbour (a tidal inlet on the southern coast of the UK) were also assessed using the same type of laboratory flume runs (Pidduck and Manning, in prep.). The same protocols used for the pre-determined mixture experiments, were adopted for these runs. Sediment transport in Portsmouth Harbour has been studied by Hydraulics Research (1959), Lonsdale (1969) and Harlow (1980). Regular dredging activities for military vessel access to the Royal Naval Base, combined with an ebb-dominant macrotidal regime, mean that the fine mud and coarser sands that reside in the Harbour can become mixed.

Two Portsmouth Harbour samples at a constant SPM concentration of 2000 $mg.l^{-1}$ and sheared at 0.35 Pa are described. The first suspension, 4_A (Fig. 10a), was a low cohesive sediment composed of 38M:62S (including coarse silts). Loss-on-ignition tests indicated that sediment 4_A was approximately 6% organic. The 4_A flocs ranged in size from 29-313 μm, although there is an absence of particles in the 33 to 69 μm range. The smallest microflocs (2% of the population) all demonstrate effective densities of quartz and beyond, which suggests the presence of some very dense minerals; possibly some metallic particles. The larger microflocs were less dense (~ 700 $kg.m^{-3}$).

The 4_A microflocs comprised just over half of the SPM, with their settling velocities spanning three orders of magnitude from 0.36-34 $mm.s^{-1}$. This resulted in a Ws_{micro} of 5.4 $mm.s^{-1}$, which was 1.3 $mm.s^{-1}$ quicker than the larger macroflocs. This was due to the macroflocs demonstrating effective densities predominantly below 200 $kg.m^{-3}$, which are more indicative of cohesive flocs.

The second sample, 6_B (Fig. 10b), was more cohesive as it contained only 30% sand (70M:30S) and the sediment mixture had 8.4% organic matter present within its matrix. Where the sample 4_A D vs. Ws distribution favoured the smaller size fractions, 6_B depicts a population more characteristic of a pure mud. The microflocs were distinctly slower in settling, ranging from

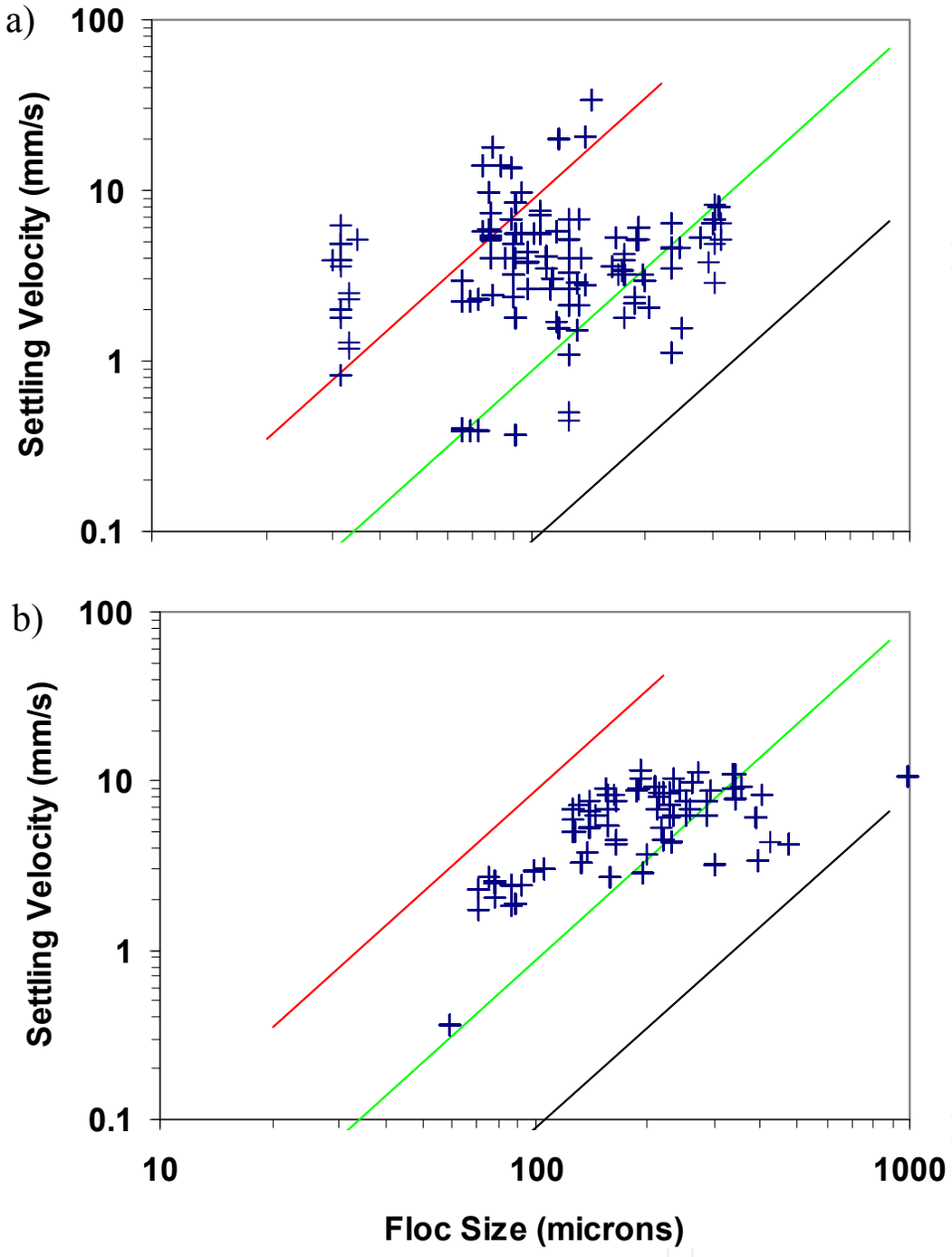

Figure 10. Settling settling vs. floc size for Portsmouth Harbour samples: a) 4_A (38M:62S); b) 6_B (38M:62S). Both samples had nominal 2 $g.l^{-1}$ total SPM concentrations and were sheared at a stress of 0.35 Pa. Diagonal lines represent contours of constant Stokes equivalent effective density: red = 1600 kgm^{-3}, green = 160 kgm^{-3}, and black = 16 kgm^{-3}.

2-8 $mm.s^{-1}$. All flocs were also less dense than 4_A; effective densities under 740 $kg.m^{-3}$, with the largest flocs having a ϱ_e of just 20 $kg.m^{-3}$.

The macroflocs comprised nearly two thirds of 6_B population and over three quarters of the mass. The macrofloc and microfloc settling dynamics of the Portsmouth Harbour samples, at

http://dx.doi.org/10.5772/55233

the three induced shear stresses (0.06, 0.35 and 0.6 Pa; 0.9 Pa was not available for the Portsmouth Harbour tests), are illustrated in Fig. 11. The data reveals some interesting settling velocity trends and these will be discussed in Section 7.

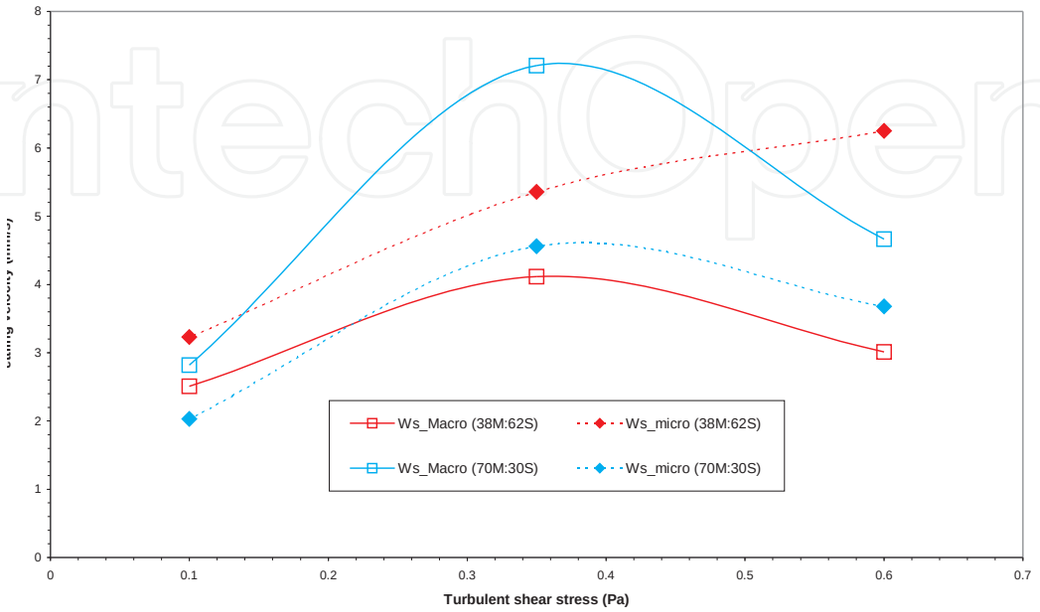

Figure 11. Ws_{macro} and Ws_{micro} values plotted against shear stress for Portsmouth Harbour samples 4_A (38M:62S) and 6_B (70M:30S). Both samples had nominal 2 $g.l^{-1}$ total SPM concentrations and were sheared at a stress of 0.35 Pa.

6.7. Floc microstructure

To illustrate how both non-cohesive and cohesive sediments components can combine in natural microflocs, electron micrographs of cross-sections through natural microflocs from the Tamar Estuary (UK) are shown in Fig. 12. The low resolution TEM image which encompasses the entire microfloc (Fig. 12a) shows the complex matrix of structurally interdependent components of a typical floc section. Both organic and inorganic particles are present creating a highly porous, high water content, three-dimensional sedimentary matrix.

7. Discussion of experimental findings

7.1. Settling velocity

This section addresses issues relating to research questions i-iii listed in Section 5. A number of generalised trends, in terms of the settling velocity, can be deduced from the macrofloc and microfloc data. The macrofloc settling velocities generally slowed as the sand content rose. These macroflocs fell slightly quicker than the microflocs at low turbidity, but almost three-times as quick at the higher suspended concentration. However, as the mud content decreased,

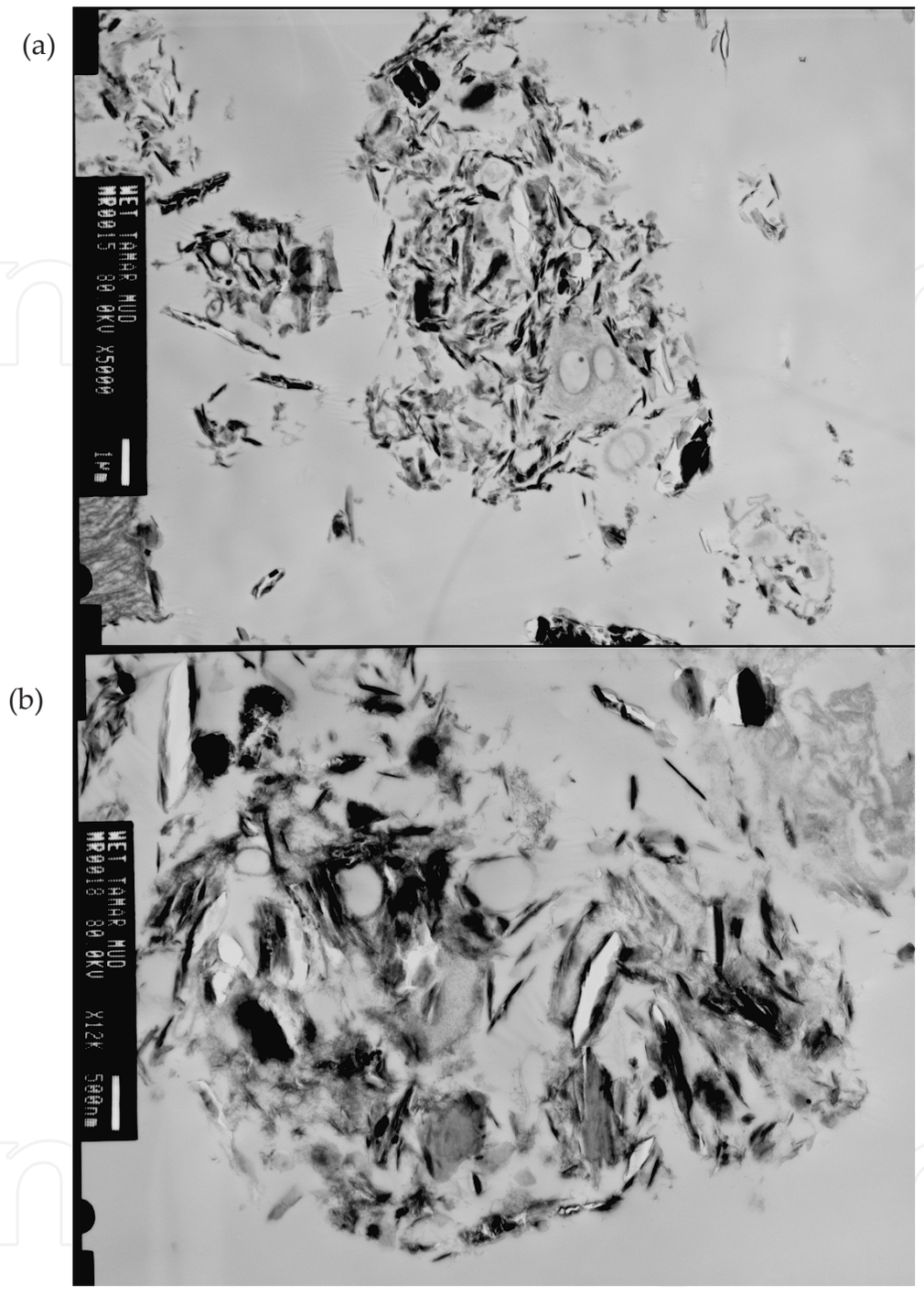

Figure 12. Low resolution (a) and high resolution (b) TEM images of a natural microfloc composed of a mud:sand mixture.

the particle cohesion efficiency would also reduce and could potentially limit the floc growth potential, curbing the equilibrium floc size of the macrofloc fraction.

The microfloc settling responded to a greater abundance of sand, whereby the greater the sand content in a mixed fraction - the faster the Ws_{micro}. For example, for a 25M:75S suspension, the microfloc settling velocities demonstrated a three-fold increase at low turbidity and nearly

http://dx.doi.org/10.5772/55233

doubled in settling speed at high turbidity to produce Ws_{micro} of 3.5 mm.s^{-1} and 4.7 mm.s^{-1}, respectively. The effective density data of many of the microfloc fractions from the pre-determined mixtures tests ranged from 800-1200 kg.m^{-3}. This would suggest that the finer sand grains tended to interact and bond better with the smaller floc structures, accounting for the quicker microfloc settling velocities observed.

The flocs produced from the natural Portsmouth Harbour sediments showed similar general settling velocity patterns to those of the pre-determined Tamar mixed suspensions. For the less cohesive 38M:62S slurry (sample 4_A), the microfloc fraction settled quicker than the macroflocs. By taking into account differences in SPM and M:S ratio, one can deduce that the 4_A microflocs were settling approximately 1.5 mm.s^{-1} quicker than their manufactured slurry equivalents, whilst the Portsmouth macroflocs fell nearly twice as quick as their pre-determined slurry equivalent. This could be a result of slightly larger sand grains present in the Portsmouth 4_A sediment and also stronger bio-film coatings present in the 4_A mixture providing extra adhesion for the sand grains permitting greater uptake within the macrofloc fraction.

It is interesting to observe that the microflocs in 4_A produced their fastest settling velocities at a τ of 0.6 Pa, whilst the Ws_{macro} peaked at a less turbulent 0.35 Pa. This can be explained by the denser microflocs being stronger than the weaker macroflocs, hence they can survive larger stresses. The ratio of a floc's diameter to the corresponding dissipating eddy size, such as the Kolmogorov microscale (1941a, b), in turbulent flow is a fundamental governing condition for estuarine flocculation dynamics (Tomi and Bagster, 1978; Tambo and Hozumi, 1979; McCave, 1984). Furthermore, if settling velocities are large, more turbulent energy is required to keep those flocs in suspension.

7.2. Composition and SPM distribution

Aspects relating to research question iv are now discussed. The LabSFLOC data has provided evidence of how sand grains can be potentially included within a floc matrix. The Ws vs. D spectra show that only a minimal amount of potentially unflocculated pure sand particles are present in a few of the samples; this is in terms of both individual numbers and the percentage of the total SPM (typically less than 1-2% of the total mud:sand concentration). An accurate mass balance between the predetermined mixed suspension introduced into the flume at the commencement of each run and the filtered SPM obtained from each sample promotes confidence in the mixed sediment LabSFLOC floc observations.

The LabSFLOC sampling protocol of measuring D and Ws simultaneously means that data on individual floc effective density is available. The latter provides important information about the composition of each floc (Dyer, 1989). The data identifies that there is a wide range in effective densities exhibited across each spectrum, particularly in the microfloc range, but most are less than pure quartz (~1600 kg.m^{-3}). Transmission electron microscopy (TEM) images have also visually identified the presence of both clay minerals and quartz mineral fragments within natural microfloc structures (Spencer et al., 2010). This leads to the suggestion that when mixed sediments flocculate, the sand particles favour the microfloc fraction, which is logical reasoning: microflocs tend to have the stronger bonding potential due to the closeness of the bonds.

Uptake of individual sand particles will probably be much less in the macroflocs. This is consistent with the order of aggregation theory (Krone, 1962; Eisma, 1986) which states that microflocs will flocculate into macroflocs when the ambient conditions are favourable. This provides a more efficient mechanism / pathway for the fine sand grains to move into the macrofloc fractions.

The EDS floc structural analysis of the TEM floc images presented in Section 6.7, identified that the microfloc inorganic constituents primarily comprised planar clay minerals (identified by the thin dark grey objects in Fig. 12) and fine quartz fragments (all much smaller than the mean sand grain size), evident from concoidal fracturing (the black marks in Fig. 12a and 12b). Other minerals present included Fe and Mn oxides and opaque sub-cubic minerals (probably pyrite), which are all typical of estuarine sediments. The organic constituents are predominantly observed to be bacteria and their EPS (extracellular polymeric substance; see Underwood and Paterson, 2003; Tolhurst et al., 2002) fibrils, which are produced by the bacteria for attachment, assimilation of food (dissolved organic carbon) and for protection from predation and contaminants. In the high resolution TEM image of the microfloc (Fig 12b.), the EPS can be seen linking the biological and inorganic particles and represents a micro-structural framework of the floc matrix (Fig. 12b). The EPS matrix is considered to be the component of the floc that enhances floc building and provides it with its strength.

For the Tamar mixtures, with a sand d_{50} of 0.11 mm, it is geometrically possible that only one sand grain may form a microfloc. The data shows that many of the microflocs exhibited effective densities significantly less than pure quartz, but higher than most pure mud microfloc. This suggests that the mixed sediment microflocs could be either combined mixtures of very fine quartz fragments and mud, as illustrated by the TEM images, or they could be individual larger quartz particles which are coated in organic mud. For example, Whitehouse et al. (2000) offer a scenario where mud can create a 'cage-work' structure which can fully encompass the sand grains, thus trapping the sand within a clay floc envelope. Mehta et al. (2009) observed flocs of various sizes in Lake Apopka (Florida, USA) where the inorganic particles are held together by embayment within a spacious exopolymeric biofilm (e.g. organic mucus) (Fig. 13). Such flocs do not conform to the mathematical fractal description typically attributed to predominantly inorganic flocs (e.g. Winterwerp and van Kesteren, 2004, Winterwerp et al, 2006), because there is no floc formation that can be described as the primary structure. All these cases would produce microflocs which are both less dense than their constituent minerals, but would have the potential to bond with a macrofloc due to their part-biological matrix.

7.3. MSF distributions

By combining the settling velocity and mass distribution findings, it is possible to assess the mass settling flux (i.e. the product of the concentration and the Ws); this enables aspects of research question v to be discussed.

The combined effects of particle concentration and turbulent shearing have long been attributed to the growth of mud flocs (e.g. Tsai et al., 1987; Burban, 1987; Puls et al., 1988; Kranck and Milligan, 1992). Under optimum flocculation conditions, Mehta and Lott (1987) suggested

http://dx.doi.org/10.5772/55233

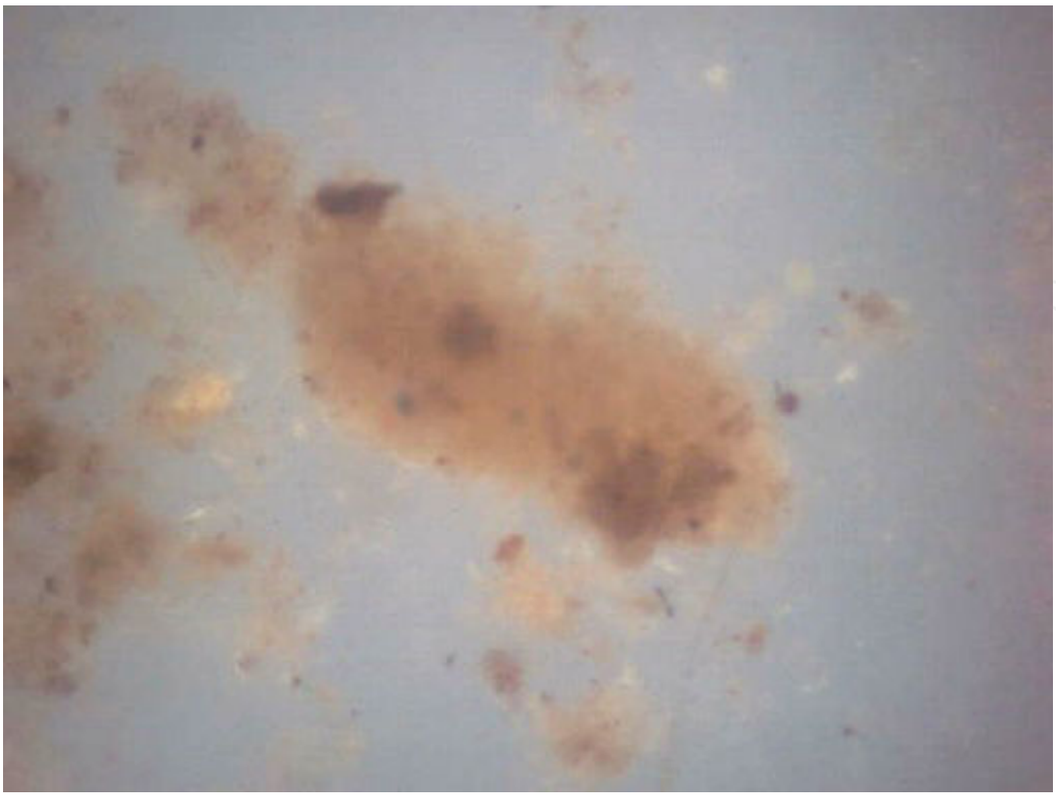

Figure 13. A very porous (low density) floc, composed from a translucent organic coating eveloping a solid (opaque) core (from Mehta et al., 2009).

that pure mud macroflocs tend to contribute most to the MSF, on account of high instability (van Leussen, 1994) due to floc growth potential producing a greater number of larger macroflocs with fast settling velocities. Observations in estuaries reveal these pure mud macroflocs can typically grow to mean a diameter > 400 μm, exhibiting effective densities of less than 40-50 $kg.m^{-3}$ and becoming more than 95% porous. These macroflocs are highly delicate entities and are easily progressively broken apart as they pass through regions of higher turbulent shear stress (Glasgow and Lucke, 1980). However, the data presented in this chapter indicates a trend whereby an increase in sand content, and a subsequent decrease in mud, favours the microflocs as the dominant flux contributor.

For example, if we consider a flocculating mixture comprising 25% mud and 75% sand, at a nominal concentration of 1000 $mg.l^{-1}$ and sheared at a τ of 0.6 Pa (i.e. Sample C6 ; see Fig. 4Civ), this results in the microflocs representing three quarters of the SPM. Therefore, the microfloc fraction would be contributing 88% of the total MSF (3.08 $g.m^{-2}s^{-1}$). To place this MSF value into perspective: it is approximately double the flux estimated for either a pure mud or a 75% mixed mud suspension; nearly 30% greater than the flux for a 50M:50S mixture; and six times greater than the MSF obtained by using a constant 0.5 $mm.s^{-1}$ settling velocity.

In contrast, by maintaining the ambient SPM concentration at 1000 $mg.l^{-1}$, but making the suspension 75% cohesive (i.e. 75M:25S), when it is sheared at 0.35 Pa (Sample A7) the total MSF (2.2 $g.m^{-2}s^{-1}$) would be weighted 73%:27% in favour of the macroflocs. This settling flux

distribution is more characteristic of a fully cohesive suspension (Manning and Bass, 2006). This suggests that with just an 8% lower MSF than pure mud, the 75M:25S mixture is behaving, to some degree, predominantly as a cohesive suspension, even with 25% fine sand present in the mixture.

The data shows that the greater the sand content of a mixed suspension, the higher the total MSF. Although it is not possible to state how much, or even when, cohesive material attaches to individual sand grains, the effective density distributions (see Figs 4Ai-v) indicate that many of the microflocs are less dense than quartz (for a nominally mass-balanced mud:sand mixture). The Ws_{micro} generally rose with rising sand content. One can see that this smaller size fraction is extremely important in terms of the total MSF for less cohesive suspensions. By averaging the MSF over the entire concentration and shear stress ranges for a nominally constant ratio of mud and sand, the data reveals that for a predominantly sandy suspension (Run C - 25M: 75S), the microflocs represented the majority (~80%) of the total MSF. In contrast, the microflocs contributed less than half (~42%) of the settling flux for the muddier 75M:25S slurry (Run A).

With the sandier 4_A Portsmouth microflocs (see Fig. 10a) representing over half of the total 2000 $mg.l^{-1}$ suspension and the macroflocs comprising three quarters of the more cohesive sample 6_B flocs (see Fig. 10b), the Portsmouth samples displayed a similar mass distribution to those of the Tamar pre-determined slurries. In terms of the MSF, Sample 4_A produced a resultant 9.9 $g.m^{-2}s^{-1}$, which was approximately 50% greater than the Tamar manufactured suspension. Whilst the Sample 6_B depositional flux, 13.6 $g.m^{-2}s^{-1}$, was more than three times the settling flux of the Tamar equivalent mixtures. The higher mass settling fluxes were a function of the quicker settling velocities demonstrated by the Portsmouth Harbour suspensions.

A direct comparison of the mass settling fluxes and their associated dynamics, can also provide a practical way to illustrate the enhanced / increased flocculation with respect to turbulent intensity. If we consider the 5000 $mg.l^{-1}$ B9 floc sample from the 50M:50S suspension, the very turbulent ($\tau = 0.9$ Pa) environment produced a net MSF of 13.8 $g.m^{-2}s^{-1}$ (see Fig. 4Ciii), with just half the flux attributed to the macroflocs. In comparison the more advanced flocculation of the less turbulent ($\tau = 0.35$ Pa) Sample B11, resulted in a MSF of 26.2 $g.m^{-2}s^{-1}$. This was nearly double the Sample B9 flux and was primarily due to the B11 macroflocs contributing 80% of the total flux. The fast settling (Ws of 6-14 $mm.s^{-1}$) macroflocs ranging from 482 to 650 μm produced nearly one quarter of the B11 MSF.

8. Parameterisation of mixed sediment flocculation

Since the mid-1990s, much research has been conducted in Europe on the parameterisation of the natural flocculation process, through projects such as COSINUS - *Prediction of COhesive Sediment transport and bed dynamics in estuaries and coastal zones with Integrated NUmerical Simulation models* (see Berlamont, 2002). A significant degree of progress has been achieved on the practical modelling of flocculation (e.g. Winterwerp et al., 2006; Baugh and Manning, 2007, Soulsby and Manning, 2012). In terms of general modelling applicability, these floccu-

lation advancements are still limited to the modelling of solely pure cohesive sediment estuaries. Due to the complexity of the mixed sediment flocculation process (as demonstrated in this chapter), statistical relationships between floc properties acquired from direct empirical observations can be used to quantify the response of flocculation to different environmental conditions (Manning and Dyer, 2007). Fig. 14 shows a conceptual representation of the 25M: 75S data compared to pure mud suspensions, at a SPM concentration of 5000 mg.l^{-1}. The mixed sediment macrofloc settling curve, within a turbulent shear stress (τ) region of 0.06-0.6 Pa, can be quantified by the following algorithm:

$$Ws_{macro} = 0.259 + 5.76*\tau - 7.61*\tau^2 + 0.000317*SPM \quad (1)$$

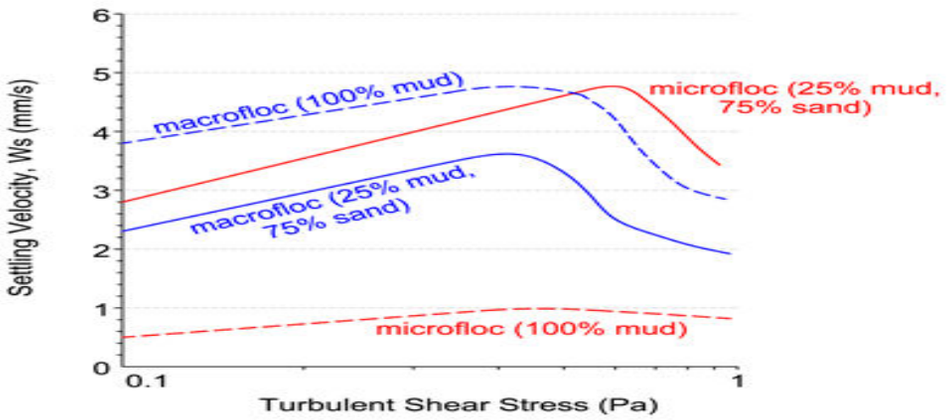

Figure 14. Conceptual illustration of Ws_{macro} (blue lines) & Ws_{micro} (red lines) trends for a mixed sediment suspension of ratio 25M:75S (solid lines) and a pure mud (dotted lines) suspension, all for a total concentration of 5 gl^{-1}, plotted against shear stress.

A parametric multiple regression was used to generate Eqn 1. For this particular type of multi-regression derivation we are using non-homogeneous dimensions, therefore the units used are as follows: Ws_{macro} = mm.s^{-1}, τ = Pa, and SPM = mg.l^{-1}. Demonstrating an R^2 = 0.84, the algorithm is a close approximation of the parameterised observations covering the 200-5000 mg.l^{-1} laboratory experimental SPM concentration range. Eqn 1 is just one form of algorithm and others can be generated from the data depending upon the modelling input variables.

The general structure of Eqn. 1 is similar to the pure mud macrofloc settling velocity relationship derived by Manning (2004a) as part of the Estuary Processes Research Project – EstProc (Estuary Process Consortium, 2005). The general shape of the Eqn. 1 curve is similar to the flocculation schematic proposed by Dyer (1989), with an increase in settling velocity at low stress due to flocculation enhanced by shear, and floc disruption at higher stresses for the same concentration. Also, the combined influence of concentration and turbulent shear on the control of the macrofloc properties, as listed in Eqn. 1, agrees with the hypotheses offered by both Puls et al. (1988) and Kranck and Milligan (1992).

However, the relative magnitudes and peaks in the mixed sediment conceptual curves (illustrated in Fig. 14) differ from the pure mud representations in a number of ways. The microflocs in the 25M:75S mixed suspension microflocs settle at a maximum velocity of 4.7 $mm.s^{-1}$; this is 380% quicker than the equivalent pure mud and nearly double the Ws_{micro} for a 75% mud suspension. Interestingly, the mixed suspension Ws_{micro} is virtually the same as the macrofloc settling velocity for pure mud. The peak 25M:75S Ws_{micro} occurred at a shear stress of 0.6 Pa, which falls within the "moderately-high" shear stress zone (Manning, 2004a); 0.2-0.3 Pa above the shear stress region typically recognised as producing optimum stimulation for pure mud flocculation (Manning, 2004a).

Manning and Dyer (2007) demonstrated that, for varying levels of suspended concentration, mud microfloc settling in turbulent flows could be represented by a single algorithm curve. In contrast, mixed sediment microfloc settling velocities appear to be dependent upon both concentration and shear stress variations, as well as the proportion of mud and sand. This is indicated by different curves representing Ws_{micro} throughout a shear stress range at varying concentration levels, even when the mud:sand ratio is constant. From this we can deduce that the mixed sediment Ws_{micro} parameter is far more sensitive to changes in SPM concentration, compared to pure mud microflocs whose dynamics only seem to vary with turbulent shear stress.

If we now examine the macrofloc settling for the conceptual curve for a 5000 $mg.l^{-1}$ 25M:75S mixed suspension (Fig. 14), one can observe that the maximum Ws_{macro} of 3.5 $mm.s^{-1}$ occurs at a shear stress of about 0.35-0.4 Pa; the same stress range as pure mud macroflocs. However, the 25M:75S macroflocs are settling 1.2 $mm.s^{-1}$ (or 25%) slower than both the Ws_{micro} peak for the mixed sediments and the Ws_{macro} for pure mud.

If we consider the mixed sediment settling velocity variations in terms of Krone's (1963) classic hierarchical order of aggregation theory, the smaller microflocs ($D < 160$ μm) are generally considered to be the building blocks from which the macroflocs are composed. The microflocs tend to display a much wider range in effective densities and settling velocities than the macrofloc fraction. It is highly plausible that for mixed sediments, the microfloc fraction samples may comprise both flocculated mud and some unflocculated sand grains depending on mud:sand ratio, concentration and shear stress. This could account for the faster microfloc settling velocities with rising sand content and concentration.

The macroflocs are deemed to be composed of microflocs, so this fraction will also contain both cohesive and non-cohesive particulates. The intra-bonding of microfloc to microfloc is usually far weaker than the closer internal particle bonds of individual microflocs. This means that macrofloc bonding relies heavily on the sediment cohesional properties (primarily those from extra-cellular polymeric substances), and these will exponentially decrease with muddy sediments being replaced by non-cohesive sands.

The parameterisation of biological process for inclusion in numerical sediment transport models is notoriously difficult, and algorithms such as Eqn. 1 do not include a specific "biological" term. However, where the algorithms are based on data derived from natural sediments which would include some of the biological effect. A limitation of many mixed

http://dx.doi.org/10.5772/55233

sediment laboratory studies, is that the mud:sand matrix is over-simplified through the use of a pure clay mineral (e.g. kaolinite) devoid of any biology. As clay minerals only flocculate through electrostatic (i.e. salt) flocculation, at best a segregated environment may be simulated if the water is brackish, but resultant mixed sediment flocculation effects will never be observed.

9. Modelling implications of mixed sediment flocculation

The prediction and modelling of mud:sand segregation effects on processes such as deposition are very useful from an estuarine management perspective. Numerical models are typically the chosen tools with which estuarine management groups attempt to predict sediment transport rates. In order for these models to provide sufficiently accurate results, a good scientific understanding of the flocculation process and interactions between mud and sand is required (e.g. Chesher and Ockenden, 1997; van Ledden, 2002; Waeles et al., 2008), and these processes need to be adequately described mathematically.

The complexity of mud:sand suspensions and a general lack of suitable experimental data which can describe the resultant dynamics of different mixtures of mud and sand, means that most numerical sediment transport models treat mud and sand as entirely separate entities. These conditions may exist for a segregational environment. However, if the mud:sand particles interact as a combined matrix, it has the potential to flocculate (as demonstrated in this chapter). This research has indicated that when mud and sand are mixed in different ratios and interact, the level of inter-particle cohesion can also vary and this is reflected in the macrofloc:microfloc mass settling flux distributions. Therefore it may be important for modellers to consider potential flocculation effects when parameterising mixed sediment deposition in turbulent flows that are conducive to flocculation.

When faced with a potential mixed sediment regime, an estuarine sediment transport modeller has two initial basic choices. The first and most simple option, is to assume that the mud:sand mixtures act solely as one sediment type when suspended, thus entirely demonstrating either cohesive or non-cohesive settling characteristics. If all sediment is assumed to be non-cohesive, e.g. pure sand grains devoid of any cohesive matter, the SPM would behave as inert particles as their dynamic settling spectrum would not alter greatly with increasing concentration as they do not flocculate. Similarly pure sand grain dynamics are not affected by shear stresses in the same way muddy sediments are. Thus, the settling properties of pure sand suspensions are similar over the SPM concentration range (200-5000 $mg.l^{-1}$) encompassed by the flume experimental data reported in this chapter; this is also because the influence of hindered settling is not important in this range of concentration. In contrast, if all SPM present is deemed to be pure mud, flocculation will completely dominate the settling process.

The second option acknowledges the presence of a mud:sand mixed environment; the issue is then how this is handled. For example, Van Ledden's (2002) mixed sediment model employed the segregational criteria for low concentration depositional simulations in which flocculation effects are ignored. However, if it is assumed that the mixed suspensions are acting in a

segregated manner, when in fact they are demonstrating a degree of flocculation, a wide range in predicted settling flux errors may arise from the modelling output.

To illustrate the potential pitfalls of solely using either a sand or mud settling parameterisation, when there is actually a flocculating mud:sand mixture present, we compare fraction-maximum settling velocities for: pure mud, pure sand and a 50M:50S ratio suspension, all at an SPM concentration of 200 $mg.l^{-1}$. For the 100% mud condition, the respective macrofloc and microfloc settling velocities are 2.4 $mm.s^{-1}$ and 0.9 $mm.s^{-1}$. The contrasting pure sand settling velocity values are Ws_{macro_sand} = 20.1 $mm.s^{-1}$ and Ws_{micro_sand} = 7.4 $mm.s^{-1}$; this was a comparative 7 to 8 -fold settling velocity rise for the two respective pure sand fractions, over the pure mud. An equal division of mud and sand resulted in an observed mixed sediment macrofloc settling velocity of 1.6 $mm.s^{-1}$, which was more than twelve times slower than the pure sand macrofloc-equivalent sized fraction and two thirds the velocity of the pure mud macroflocs. However, the observed 50M:50S microflocs fell at 2.2 $mm.s^{-1}$, which was three-times slower than pure sand, and twice as fast as pure mud suspensions. This example demonstrates the importance of obtaining high quality temporal and spatial settling velocity data of mixed sediments in suspension. It is anticipated that the effects of mixed sediment flocculation on numerical sediment transport modelling, will be the topic of future research and publication.

10. Conclusion

The aim of this chapter was to provide an overview of mixed sediment flocculation dynamics and how they can influence sediment transport. It has drawn on key literature and new data to address this aim. The theoretical aspects relating to the flocculation of mud:sand mixtures include flocculation processes, segregation versus flocculating suspensions, and biological influences on mixed sediment flocculation.

In order to demonstrate the flocculation potential and characteristics of mud:sand mixtures, the second part of the chapter has drawn on the findings from recently completed laboratory studies that examined the flocculation dynamics for mud:sand (M:S) mixtures primarily using Tamar estuary mud and silica sand at different concentrations and shear rates in a mini-annular flume. Turbulent shear stresses during the experimental runs ranged from 0.06-0.9 Pa (±5%), with maximum flow speeds in the annular flume of about 0.7 $m.s^{-1}$, for three total suspended sediment concentrations representative of estuarine concentrations, namely 200, 1000 and 5000 $mg.l^{-1}$. The video-based LabSFLOC instrument was used to determine floc properties including size, settling velocity, density, and mass.

The experiments showed that as mud content decreased, the particle cohesion efficiency reduces which can limit the growth potential of the macrofloc fraction (sizes > 160 μm). For a 75M:25S suspension, the settling velocity Ws_{macro} was slightly quicker than the microflocs at 200 $mg.l^{-1}$, but almost three-times as fast at the higher suspended concentration (5000 $mg.l^{-1}$). Parameterised data indicated that by adding more sand to a mud:sand mixture, the settling velocity of the macrofloc fraction slows and the settling velocity of microflocs (sizes < 160 μm) increases.

http://dx.doi.org/10.5772/55233

In terms of floc composition, effective density data of many of the microfloc fractions ranged between 800-1200 $kg.m^{-3}$. This would suggest that the finer sand grains tended to interact and bond better with the smaller floc structures, accounting for the quicker microfloc settling velocities observed.

The general trends revealed by the pre-determined (Tamar mud and silica) mixtures were also observed with independent tests on naturally mixed Portsmouth Harbour sediments. However, compositionally, the Portsmouth sediment matrix produced differences in the absolute settling velocities of the macrofloc and microfloc fractions from those of the Tamar mixtures. Both fractions of the Portsmouth sediment tended to fall quicker than their Tamar mixed sediment equivalents. It is proposed that this could be a result of a different sand grain size distribution combined with stronger bio-film coatings producing added cohesion in the Portsmouth sediment mixtures. This would permit a greater uptake of the sand grains within the macrofloc fraction, whilst also potentially forming the faster settling microflocs observed.

The data showed that the greater the sand content of a mixed suspension, the higher the total mass settling flux (MSF). As the microflocs have been seen to be more conducive at flocculating with the finer sand grains, and the Ws_{micro} rose with rising sand content, one can see that this smaller size fraction is extremely important in terms of the total MSF for less muddy suspensions. By averaging the MSF over the entire concentration and shear stress ranges for a constant ratio of mud (M) and sand (S), the data revealed that for a predominantly sandy suspension (25M:75S), the microflocs represented the majority of the total MSF. In contrast, the microflocs contributed less than half of the settling flux for a much muddier mixture (75M:25S).

Biology is considered to be extremely important in the mixed sediment flocculation process. For example, the presence of sticky extracellular polymeric substances (EPSs) produced by epipelic and epipsammic diatoms could significantly enhance particle bonding. Energy dispersive spectroscopy analysis confirmed the presence of both clay minerals and quartz mineral fragments within a natural microfloc. A high resolution transmission electron microscopy (TEM) image revealed EPS fibrils linking the biological and inorganic particles within a micro-structural framework of a microfloc matrix.

Since estuaries may have mixed or segregational mud:sand environments and numerical models are used to inform management decisions, some issues relating to the parameterisation of mud:sand flocculation and their implementation in sediment transport models have been discussed. It is anticipated that these two topics will be the subject of future research and publication on mixed sediment flocculation.

Acknowledgements

The mini-annular flume experiments were primarily funded by the HR Wallingford Company Research Programme as part of the 'Mud:Sand Transport' projects (DDD0301 and DDD0345), and completed during the 'Sediment in Transitional Environments' – SiTE project (DDY0427).

Author details

Andrew J. Manning[1,2], Jeremy R. Spearman[1], Richard J.S. Whitehouse[1], Emma L. Pidduck[2], John V. Baugh[1] and Kate L. Spencer[3]

1 HR Wallingford, Howbery Park, Wallingford, Oxfordshire, UK

2 School of Marine Science & Engineering, University of Plymouth, Plymouth, Devon, UK

3 Department of Geography, Queen Mary – University of London, Mile End Road, London, UK

References

[1] Alvarez-Hernandez, E. (1990). The influence of cohesive sediment on sediment movement in channels of circular cross-section. PhD thesis, University of Newcastle-upon-Tyne.

[2] Bass, S.J., Manning, A.J. and Dyer, K.R. (2006). Preliminary findings from a study of the upper reaches of the Tamar Estuary, UK, throughout a complete tidal cycle: Part I. Linking sediment and hydrodynamic cycles. In: J.P.-Y. Maa, L.P. Sanford and D.H. Schoellhamer (eds), Coastal and Estuarine Fine Sediment Processes - Proc. in Marine Science 8, Amsterdam: Elsevier, pp. 1-14, ISBN: 0-444-52238-7.

[3] Baugh, J.V. and Manning, A.J. (2007). An assessment of a new settling velocity parameterisation for cohesive sediment transport modelling. Continental Shelf Research, doi:10.1016/j.csr.2007.03.003.

[4] Berlamont, J.E. (2002). Prediction of cohesive sediment transport and bed dynamics in estuaries and coastal zones with integrated numerical simulation models. In: Winterwerp, J.C., Kranenburg, C. (eds), Fine Sediment Dynamics in the Marine Environment - Proc. in Mar. Sci. 5., Elsevier, Amsterdam, pp. 1-4.

[5] de Brouwer, J.F.C., Wolfstein, K., Ruddy, G.K. (2005). Biogenic stabilization of intertidal sediments: The importance of extracellular polymeric substances produced by benthic diatoms. Microbial Ecology, 49, 501-512.

[6] Buffle, J. and Leppard, G.G. (1995). Characterisation of aquatic colloids and macromolecules. 2. Key role of physical structures on analytical results. Environmental Science and Technology, 29, 2176-2184.

[7] Burban, P.Y. (1987). The flocculation of fine-grained sediments in estuarine waters. MSc. thesis, Dep. of Mech. Eng. Univ. of Calif., Santa Barbara, USA.

[8] Cahoon, L.B. (1999). The role of benthic microalgae in neritic ecosystems. Oceanography and marine biology: an annual review, 37, 47-86.

[9] Chesher, T.J. and Ockenden, M.C. (1997). Numerical modelling of mud and sand mixtures. In: N. Burt, R. Parker and J. Watts (Eds), Cohesive Sediments – Proc. of INTERCOH Conf. (Wallingford, England), Chichester: John Wiley & Son, pp. 395-406.

[10] Dankers, P.J.T., Sills, G.C. and Winterwerp, J.C. (2007). On the hindered settling of highly concentrated mud-sand mixtures. In: T. Kudusa, H. Yamanishi, J. Spearman and J.Z. Gailani (Eds), Sediment and Ecohydraulics - Proc. in Marine Science, INTERCOH 2005, Amsterdam: Elsevier, pp. 255-274.

[11] Dearnaley, M.P. (1996). Direct measurements of settling velocities in the Owen Tube: a comparison with gravimetric analysis. Journal of Sea Research, Vol. 36, Nos. 1-2, 36, 41-47.

[12] Dyer, K.R. (1986). Coastal and Estuarine Sediment Dynamics. Wiley & Sons, Chichester, 342p.

[13] Dyer, K.R. 1989. Sediment processes in estuaries: future research requirements. J. Geophys. Res., 94 (C10): 14,327-14,339.

[14] Dyer, K.R., Cornelisse, J.M., Dearnaley, M., Jago, C., Kappenburg, J., McCave, I.N., Pejrup, M., Puls, W., van Leussen, W. and Wolfstein, K. (1996). A comparison of in-situ techniques for estuarine floc settling velocity measurements. Journal of Sea Research 36, 15-29.

[15] Dyer, K.R. and Manning, A.J. (1998). Observation of the size, settling velocity and effective density of flocs, and their fractal dimensions. Journal of Sea Research 41, 87-95.

[16] Edzwald, J.K. and O'Melia, C.R. (1975). Clay distributions in recent estuarine sediments. Clays and Clay Minerals, 23:39-44.

[17] Eisma, D. (1986). Flocculation and de-flocculation of suspended matter in estuaries. Neth. J. Sea Res., 20 (2/3), 183-199.

[18] Estuary Process Consortium (2005). Final Report of the Estuary Process Research Project (EstProc) – Algorithms and Scientific Information. Integrated Research Results on Hydrobiosedimentary Processes in Estuaries, R & D Technical Report prepared by the Estuary Process Consortium for the Fluvial, Estuarine and Coastal Processes Theme, co-funded by Defra & Environment Agency, Report FD1905/TR3, 140p.

[19] Feates, N.G. and Mitchener, H.J. (1998). Properties of dredged material: measurement of sediment properties of dredged material from Harwich Harbour. HR Wallingford Report TR 46.

[20] Fennessy, M.J., Dyer, K.R. and Huntley, D.A. (1994). Size and settling velocity distributions of flocs in the Tamar Estuary during a tidal cycle. Netherlands Journal of Aquatic Ecology, 28: 275-282.

[21] Fennessy, M.J., Dyer, K.R., Huntley, D.A. and Bale, A.J. (1997). Estimation of settling flux spectra in estuaries using INSSEV. In: N. Burt, R. Parker and J. Watts (Eds), Cohesive Sediments – Proc. of INTERCOH Conf. (Wallingford, England), Chichester: John Wiley & Son, pp. 87-104.

[22] Fitzpatrick, F. (1991). Studies of sediments in a tidal environment. Ph.D. Thesis, Department of Geological Sciences, University of Plymouth, 221p.

[23] Förstner, U. and Wittmann G. T. W. (1983). Metal Pollution in the Aquatic Environment. Springer Verlag, Berlin, Heidelberg et New York, 2nd revised edition, 486p.

[24] Gerbersdorf, S.U., Bittner, R., Lubarsky, H., Manz, W. and Paterson, D.M. (2009). Microbial assemblages as ecosystem engineers of sediment stability. J Soils Sediments, 9, 640–652.

[25] Grabowski, R.C., Droppo, I.G. and Wharton, G. (2011). Erodibility of cohesive sediment: The importance of sediment properties. Earth-Science Reviews, 105, 101-120.

[26] Glasgow, L.A. and Lucke, R.H. (1980). Mechanisms of deaggregation for clay-polymer flocs in turbulent systems. Ind. Eng. Chem. Fundam., 19: 148-156.

[27] Gratiot, N. and Manning, A.J. (2004). An experimental investigation of floc characteristics in a diffusive turbulent flow. In: P. Ciavola and M. B. Collins (Eds), Sediment Transport in European Estuaries, Journal of Coastal Research, SI 41, 105-113.

[28] Harlow, D. (1980). Sediment Processes, Selsey Bill to Portsmouth, PhD thesis, Department of Civil Engineering, University of Southampton.

[29] Harper, M.A. and Harper, J.F. (1967). Measurements of diatom adhesion and their relationship with movement. British Phycological Bulletin, 3, 195-207.

[30] Hickman, M. and Round, F.E. (1970). Primary production and standing crops of epipsammic and epipelic algae. British Phycological Journal, Vol 5 (2), pp. 247-255.

[31] HR Wallingford (1998). SandCalc: Marine Sands Calculator Interface. Version 2.0 for Windows. Software by Tessela & HR Wallingford.

[32] Hydraulics Research (1959). Portsmouth harbour investigation, parts i and ii. Reports 213b and 214, Technical report, Hydraulics Research.

[33] Kamphuis, W and Hall, K.R. (1983). Cohesive material erosion by unidirectional current. J. Hyd. Eng., ASCE, 109, 49-61.

[34] Kennish, M.J. (1986). "Ecology of estuaries Volume 1: Physical and chemical aspects." Boca Raton Florida, CRC Press, 1.

[35] Koglin B. (1977). Assessment of the degree of aggregation in suspension. Powder Technology 17, 219-227.

[36] Klimpel R.C. and Hogg R. (1986). Effects of flocculation conditions on agglomerate structure. Journal of Colloid Interface Science 113, 121-131.

[37] Kolmogorov, A.N. (1941a). The local structure of turbulence in incompressible viscous fluid for very large Reynolds numbers. C. R. Acad. Sci. URSS, 30: 301.

[38] Kolmogorov, A.N. (1941b). Dissipation of energy in locally isotropic turbulence. C. R. Acad. Sci. URSS, 32: 16.

[39] Kranck, K. and Milligan, T.G. (1992). Characteristics of suspended particles at an 11-hour anchor station in San Francisco Bay, California. Journal of Geophysical Research, 97, 11373-11382.

[40] Krone, R.B. (1962). Flume studies of the transport of sediment in estuarial shoaling processes. Final report. Hyd. Eng. Lab. and Sanitary Eng. Lab., University of California, Berkeley.

[41] Krone, R. B. (1963). A study of rheological properties of estuarial sediments. Report No. 63-68, Hyd. Eng. Lab. and Sanitary Eng. Lab., University of California, Berkeley, 63-68.

[42] Little, C. (2000). The biology of soft shores and estuaries. Oxford University Press (UK), 252p., ISBN: 978-0-19850-426-9.

[43] Lonsdale, B. J. (1969). A sedimentary study of the eastern Solent, Master's thesis, Department of Oceanography, University of Southampton.

[44] Manning, A.J. (2001). A study of the effects of turbulence on the properties of flocculated mud. Ph.D. Thesis. Institute of Marine Studies, University of Plymouth, 282p.

[45] Manning, A.J. (2004a). The observed effects of turbulence on estuarine flocculation. In: P. Ciavola and M. B. Collins (eds), Sediment Transport in European Estuaries, Journal of Coastal Research, SI 41, 90-104.

[46] Manning, A.J. (2004b). Observations of the properties of flocculated cohesive sediment in three western European estuaries. In: P. Ciavola and M. B. Collins (Eds), Sediment Transport in European Estuaries, Journal of Coastal Research, SI 41, 70-81.

[47] Manning, A.J. (2006). LabSFLOC – A laboratory system to determine the spectral characteristics of flocculating cohesive sediments. HR Wallingford Technical Report, TR 156.

[48] Manning, A.J., Bass, S.J. and Dyer, K.R. (2006). Floc Properties in the Turbidity Maximum of a Mesotidal Estuary During Neap and Spring Tidal Conditions. Marine Geology, 235, 193-211.

[49] Manning, A.J., Baugh, J.V., Spearman, J. and Whitehouse, R.J.S. (2009). Flocculation Settling Characteristics of Mud:Sand Mixtures. Ocean Dynamics, PECS2008 SI, DOI: 10.1007/s10236-009-0251-0.

[50] Manning, A.J. and Dyer, K.R. (1999). A laboratory examination of floc characteristics with regard to turbulent shearing. Marine Geology 160, 147-170.

[51] Manning, A.J. and Dyer, K.R. (2002a). The use of optics for the in-situ determination of flocculated mud characteristics. J. Optics A: Pure and Applied Optics, Institute of Physics Publishing, 4, S71-S81.

[52] Manning, A.J. and Dyer, K.R. (2002b). A comparison of floc properties observed during neap and spring tidal conditions. In: J.C. Winterwerp and C. Kranenburg (Eds), Fine Sediment Dynamics in the Marine Environment - Proc. in Marine Science 5, Amsterdam: Elsevier, pp. 233-250, ISBN: 0-444-51136-9.

[53] Manning, A.J. and Dyer, K.R. (2007). Mass settling flux of fine sediments in Northern European estuaries: measurements and predictions. Marine Geology, 245, 107-122, doi:10.1016/j.margeo.2007.07.005.

[54] Manning, A.J., Spearman, J. and Whitehouse, R.J.S. (2007). Mud:Sand Transport – Flocculation & Settling Dynamics within Turbulent Flows, Part 1: Analysis of laboratory data. HR Wallingford Internal Report, IT 534, 32p.

[55] Manning, A.J. and Whitehouse, R.J.S. (2009). UoP Mini-annular flume – operation and hydrodynamic calibration. HR Wallingford Technical Report, TR 169.

[56] McCave, I.N. (1984). Size spectra and aggregation of suspended particles in the deep ocean. Deep-Sea Res., 31: 329-352.

[57] Mehta, A.J., Jaeger, J.M., Valle-Levinson, A., Hayter, E.J., Wolanski, E. and Manning, A.J. (2009). Resuspension Dynamics in Lake Apopka, Florida. Final Synopsis Report, submitted to St. Johns River Water Management District, Palatka, Florida, June 2009, Report No. UFL/COEL-2009/00, 158p.

[58] Mehta, A.J. and Lott, J.W. (1987). Sorting of fine sediment during deposition. Proc. Speciality Conf. Advances in Understanding Coastal Sediment Processes. Am. Soc. Civ. Eng., New York, pp. 348-362.

[59] Mietta, F. (2010). Evolution of floc size distribution of cohesive sediments. Ph.D. Thesis, Delft University of Technology, Faculty of Civil Engineering and Geosciences, The Netherlands, 169p.

[60] Migniot, C. (1968). Study of the physical properties of various very fine sediments and their behaviour under hydrodynamic action. La Houille Blanche, 23 (7). (Translation of French text).

[61] Mitchener, H.J., Torfs, H. and Whitehouse, R.J.S. (1996). Erosion of mud/sand mixtures. Coastal Engineering, 29, 1-25 [Errata, 1997, 30, 319].

[62] Mory, M., Gratiot, N., Manning, A.J. and Michallet, H. (2002). CBS layers in a diffusive turbulence grid oscillation experiment. In: J.C. Winterwerp and C. Kranenburg (Eds.), Fine Sediment Dynamics in the Marine Environment - Proc. in Mar. Science 5, Amsterdam: Elsevier, pp.139-154, ISBN: 0-444-51136-9.

[63] Nowell, A.R.M., Jumars, P.A. and Eckman, J.E. (1981). Effects of biological activities on the entrainment of marine sediments. Mar. Geol., 42, 133-153.

[64] Ockenden, M.C. and Delo, E.A. (1988). Consolidation and erosion of estuarine mud and sand mixtures – an experimental study. HR Wallingford Report, SR 149.

[65] Owen, M.W. (1976). Determination of the settling velocities of cohesive muds. Hydraulics Research, Wallingford, Report No. IT 161, 8p.

[66] Panagiotopoulus, I., Voulgaris, G. and Collins, M.B. (1997). The influence of clay on the threshold of movement of fine sandy beds. Coastal Eng., 32, 19-43.

[67] Parker, D.S., Kaufman, W.J. and Jenkins, D. (1972). Floc break-up in turbulent flocculation processes. J. Sanitary Eng. Div., Proc. Am. Soc. Civil Eng., 98 (SA1): 79-97.

[68] Paterson, D.M. (1989). Short-term changes in the erodibility of intertidal cohesive sediments related to the migratory behaviour of epipelic diatoms. Limnol. Oceanogr. 34: 223-234.

[69] Paterson, D.M., Crawford, R.M. and Little, C. (1990). Subaerial exposure and changes in the stability of intertidal estuarine sediments. Estuarine Coastal and Shelf Science, 30, 541-556.

[70] Paterson, D.M. and Hagerthey, S.E. (2001). Microphytobenthos in contrasting coastal ecosystems: Biology and dynamics. In: Ecological comparisons of sedimentary shores (K. Reise, Ed.), Ecological studies, pp. 105-125.

[71] Pidduck, E.L. and Manning, A.J., in prep. A Laboratory Examination of Flocculation Properties Exhibited by Natural Sediment Mixtures from Portsmouth Harbour, UK. HR Wallingford Technical Report, TR 182.

[72] Puls, W., Kuehl, H. and Heymann, K. (1988). Settling velocity of mud flocs: results of field measurements in the Elbe and the Weser Estuary. In: J. Dronkers, and W. van Leussen, (eds), Physical Processes in Estuaries. Berlin: Springer-Verlag, pp. 404-424.

[73] Raudkivi, A.J. (1998). Loose boundary hydraulics. 3rd Edition. Balkema, Rotterdam.

[74] Reid, G.K. and Wood, R.D. (1976). "Ecology of inland water and estuaries." New York: D. Van Nostrand Company.

[75] Soulsby, R.L. and Manning, A.J. (2012). Cohesive sediment settling flux: settling velocity of flocculated mud. Technical Note DDY0409-01, HR Wallingford, Wallingford, UK.

[76] Spearman, J.R., Manning, A.J. and Whitehouse, R.J.S. (2011). The settling dynamics of flocculating mud:sand mixtures: Part 2 – Numerical modelling. Ocean Dynamics, INTERCOH 2009 special issue, DOI: 10.1007/s10236-011-0385-8.

[77] Spencer, K.L., Manning, A.J., Droppo, I.G., Leppard, G.G. and Benson, T. (2010). Dynamic interactions between cohesive sediment tracers and natural mud. Journal of Soils and Sediments, Volume 10 (7), doi:10.1007/s11368-010-0291-6.

[78] Tambo, N. and Hozumi, H. (1979). Physical characteristics of flocs – II. Strength of flocs. Water Research, 13, 409-419.

[79] Tambo, N. and Watanabe, Y., (1979). Physical characteristics of flocs-I. The floc density function and aluminium floc. Water Research 13, 409-419.

[80] ten Brinke, W.B.M. (1993). The impact of biological factors on the deposition of fine grained sediment in the Oosterschelde (The Netherlands). Ph.D. Thesis, University of Utrecht, The Netherlands, 252p.

[81] Tolhurst, T.J., Gust. G. and Paterson, D.M. (2002). The influence on an extra-cellular polymeric substance (EPS) on cohesive sediment stability. In: J.C. Winterwerp and C. Kranenburg (Eds), Fine Sediment Dynamics in the Marine Environment - Proc. in Marine Science 5, Amsterdam: Elsevier, pp. 409-425, ISBN: 0-444-51136-9.

[82] Tomi, D.T., Bagster, D.F. (1978). The behaviour of aggregates in stirred vessels: Part I - Theoretical considerations on the effects of agitation. Trans. Inst. Chem. Eng., 56, 1-8.

[83] Torfs, H. (1994). Erosion of layered sand-mud beds in uniform flow. Proc. 24th Int. Conf. Coastal Eng., Kobe, Japan, 23-28 October 1994.

[84] Torfs, H., Mitchener, H.J., Huysentruyt, H. and Toorman, E. (1996). Settling and consolidation of mud/sand mixtures. Coastal Engineering, 29, 27-45.

[85] Tsai, C.H., Iacobellis, S. and Lick, W. (1987). Flocculation of fine-grained sediments due to a uniform shear stress. J. Great Lakes Res., 13: 135-146.

[86] Uncles, R.J., Stephens, J.A. and Harris, C. (1998). Seasonal variability of subtidal and intertidal sediment distributions in a muddy, macrotidal estuary: the Humber-Ouse, UK. In: Sedimentary Processes in the Intertidal Zone, Black, K.S., Paterson, D.M. and Cramp, A. (Eds), Geological Society, London, Special Publications, 139, 211-219.

[87] Underwood, G.J.C. and Kromkamp, J. (1999). Primary production by phytoplankton and microphytobenthos in estuaries. Advances in ecological research, 29, 93-153.

[88] Underwood, G.J.C. and Paterson, D.M. (2003). The importance of extracellular carbohydrate production by marine epipelic diatoms. Advances in Botanical Research (incorporating Advances in Plant Pathology), Vol. 40, Elsevier, Amsterdam, pp.183-240, ISBN: 0-12-005940-1.

[89] Van de Ven, T.G. and Hunter, R.J. (1977). The energy dissipation in sheared coaggulated soils. Rheologica Acta, 16, 534-543.

[90] van Ledden, M. (2002). A process-based sand-mud model. In: J.C. Winterwerp and C. Kranenburg (Eds.), Fine Sediment Dynamics in the Marine Environment - Proc. in Mar. Science 5, Amsterdam: Elsevier, pp.577-594, ISBN: 0-444-51136-9.

[91] van Ledden, M. (2003). Sand-mud segregation in estuaries and tidal basins. Ph.D. Thesis, Delft University of Technology, The Netherlands, Report No. 03-2, ISSN 0169-6548, 217p.

[92] van Leussen, W. (1988). Aggregation of particles, settling velocity of mud flocs: a review. In: Dronkers, J., van Leussen, W. (Eds), Physical Processes of Estuaries, Berlin: Springer, pp. 347-403.

[93] van Leussen, W. (1994). Estuarine macroflocs and their role in fine-grained sediment transport. Ph.D. Thesis, University of Utrecht, The Netherlands, 488p.

[94] van Wijngaarden, M., Venema, L.B., De Meijer, R.J., Zwolsman, J.J.G., Van Os, B. and Gieske, J.M.J. (2002a). Radiometric sand-mud characterisation in the Rhine-Meuse estuary, Part A: Fingerprinting. Geomorphology, 43, 87-101.

[95] van Wijngaarden, M., Venema, L.B., and De Meijer, R.J. (2002b). Radiometric sand-mud characterisation in the Rhine-Meuse estuary, Part B: In situ mapping. Geomorphology, 43, 103-116.

[96] Waeles, B., Le Hir, P. and Lesueur, P. (2008). A 3D morphodynamic process-based modelling of a mixed sand/mud coastal environment : the Seine Estuary, France. In: T. Kudusa, H. Yamanishi, J. Spearman and J.Z. Galiani, (eds.), Sediment and Ecohydraulics - Proc. in Marine Science 9, Amsterdam: Elsevier, pp. 477-498, ISBN: 978-0-444-53184-1.

[97] Whitehouse, R.J.S., Soulsby, R., Roberts, W. and Mitchener, H.J. (2000). Dynamics of Estuarine Muds. Thomas Telford Publications, London, 232p.

[98] Widdows, J., Blauw, A., Heip, C.H.R., Herman., P.M.J., Lucas, C.H., Middelburg, J.J., Schmidt, S., Brinsley, M.D., Twisk, F. and Verbeek, H. (2004). Role of physical and biological processes in sediment dynamics of a tidal flat in Westerschelde Estuary, SW Netherlands. Mar. Ecol. Prog. Series, 274, 41-56.

[99] Williamson, H.J. (1991). Tidal transport of mud / sand mixtures: Sediment distributions – a literature review. HR Wallingford, Report SR 286.

[100] Williamson, H.J. and Ockenden, M.C. (1993). Laboratory and field investigations of mud and sand mixtures. In: Sam S.Y Wang (Ed.), Advances in Hydro-science and Engineering, Proceedings of the First International Conference on Hydro-science and Engineering, Washington D.C. (7-11 June 1993), volume 1, pp. 622-629.

[101] Winterwerp, J. C. (1998). A simple model for turbulence induced flocculation of cohesive sediment, J. Hyd. Eng., 36 (3), 309-326.

[102] Winterwerp, J.C. and van Kesteren, W.G.M. (2004). Introduction to the physics of cohesive sediment in the marine environment. Developments in Sedimentology, 56, van Loon, T. (Ed.), Amsterdam: Elsevier, 466p.

[103] Winterwerp, J.C., Manning, A.J., Martens, C., de Mulder, T., and Vanlede, J. (2006). A heuristic formula for turbulence-induced flocculation of cohesive sediment. Estuarine, Coastal and Shelf Science, 68, 195-207.

[104] Wolanski, E. (2007). Estuarine Ecohydrology. Elsevier (Amsterdam, The Netherlands), 157p, ISBN: 978-0-444-53066-0.